ปฏิกิริยาคาร์บอนไดออกไซด์รีฟอร์มมิ่งของมีเทน สำหรับการผลิตไฮโดรเจน บนตัวเร่งปฏิกิริยาโคบอลต์และนิกเกิล-โคบอลต์

นางสาววราลี มารุ่งเรือง

วิทยานิพนธ์นี้เป็นส่วนหนึ่งของการศึกษาตามหลักสูตรปริญญาวิศวกรรมศาสตรมหาบัณฑิต
สาขาวิชาวิศวกรรมเคมี ภาควิชาวิศวกรรมเคมี
คณะวิศวกรรมศาสตร์ จุฬาลงกรณ์มหาวิทยาลัย
ปีการศึกษา 2556

CARBON DIOXIDE REFORMING OF METHANE FOR HYDROGEN PRODUCTION ON CO CATALYSTS AND NI-CO BIMETALLIC CATALYSTS

Miss Waralee Marungrueang

A Thesis Submitted in Partial Fulfillment of the Requirements
for the Degree of Master of Engineering Program in Chemical Engineering
Department of Chemical Engineering
Faculty of Engineering
Chulalongkorn University
Academic Year 2013

Thesis Title	CARBON DIOXIDE REFORMING OF METHANE FOR HYDROGEN PRODUCTION ON CO CATALYSTS AND NI-CO BIMETALLIC CATALYSTS
By	Miss Waralee Marungrueang
Field of Study	Chemical Engineering
Thesis Advisor	Assistant Professor Suphot Phatanasri, D.Eng.

Accepted by the Faculty of Engineering, Chulalongkorn University in Partial Fulfillment of the Requirements for the Master's Degree

.....Dean of the Faculty of Engineering
(Professor Bundhit Eua-Arporn, Ph.D.)

THESIS COMMITTEE

.....Chairman
(Assistant Professor Montree Wongsri, D.Sc.)

.....Thesis Advisor
(Assistant Professor Suphot Phatanasri, D.Eng.)

.....Examiner
(Associate Professor Joongjai Panpranot, Ph.D.)

.....External Examiner
(Assistant Professor Soipatta Soisuwan, D.Eng.)

วราลี มารุ่งเรือง : ปฏิกิริยาคาร์บอนไดออกไซด์รีฟอร์มมิ่งของมีเทน สำหรับการผลิตไฮโดรเจน บนตัวเร่งปฏิกิริยาโคบอลต์และนิกเกิล-โคบอลต์ (CARBON DIOXIDE RFORMING OF METHANE FOR HYDROGEN PRODUCTION ON CO CATALYSTS AND NI-CO BIMETALLIC CATALYSTS) อ.ที่ปรึกษาวิทยานิพนธ์หลัก: ผศ.ดร. สุพจน์ พัฒนะศรี, 80 หน้า.

งานวิจัยนี้มีจุดประสงค์เพื่อทำการศึกษาตัวเร่งปฏิกิริยาที่ถูกเตรียมโดยวิธีการเคลือบฝังแบบเปียก ได้แก่ ชนิดโลหะเดี่ยว คือ โคบอลต์บนตัวรองรับอะลูมินา ที่อัตราส่วนโลหะโคบอลต์เท่ากับ 7%, 10% และ 15% และตัวเร่งปฏิกิริยาชนิดโลหะคู่ คือ โคบอลต์-นิกเกิลบนตัวรองรับอะลูมินาที่อัตราส่วนโลหะนิกเกิล-โคบอลต์ เท่ากับ 3.5%-3.5%, 5%-5%, 7%-7%, 10%-10% และ 15%-15% ในปฏิกิริยามีเทนรีฟอร์มมิ่งด้วยก๊าซคาร์บอนไดออกไซด์สำหรับการผลิตไฮโดรเจนและก๊าซสังเคราะห์ ซึ่งสำหรับในงานวิจัยนี้ จะทำปฏิกิริยาที่อุณหภูมิ 700 องศาเซลเซียส ณ ความดันบรรยากาศ โดยป้อนสารตั้งต้น คือ ก๊าซผสมระหว่างมีเทนและคาร์บอนไดออกไซด์ในอัตราส่วน 1:1 จากผลการทดลองพบว่าหลังจาก120 นาทีของปฏิกิริยา ตัวเร่งปฏิกิริยาที่ได้ค่าร้อยละการเปลี่ยนแปลงของมีเทนที่ดีที่สุดในงานทดลองนี้ คือที่ปริมาณโคบอลต์ 10% สำหรับตัวเร่งปฏิกิริยาชนิดโลหะเดี่ยว และที่ปริมาณอัตราส่วน10%นิกเกิล-10%โคบอลต์ สำหรับตัวเร่งปฏิกิริยาชนิดโลหะคู่ คือ ร้อยละ 61.86 และ ร้อยละ 96.83 ตามลำดับ นอกจากนี้ยังทำการศึกษาผลของการเติมตัวสนับสนุน คือ โลหะโพแทสเซียมเข้าไปในตัวเร่งปฏิกิริยาชนิดโลหะคู่ที่อัตราส่วนโลหะนิกเกิล-โคบอลต์เท่ากับ 10%-10% ซึ่งพบว่าได้ค่าร้อยละการเปลี่ยนแปลงของมีเทนลดลงจากตัวเร่งปฏิกิริยาที่ไม่ได้เติมตัวสนับสนุนเพียงเล็กน้อย แต่ปริมาณคาร์บอนที่เกิดขึ้นลดลงอย่างเห็นได้ชัด

ภาควิชา วิศวกรรมเคมี ลายมือชื่อนิสิต .....

สาขาวิชา วิศวกรรมเคมี ลายมือชื่อ อ.ที่ปรึกษาวิทยานิพนธ์หลัก .....

ปีการศึกษา 2556

5470536321 : MAJOR CHEMICAL ENGINEERING
KEYWORDS : DRY REFORMING / BIMETALLIC CATALYSTS / COBALT CATALYSTS / HYDROGEN PRODUCTION

WARALEE MARUNGRUEANG : CARBON DIOXIDE REFORMING OF METHANE FOR HYDROGEN PRODUCTION ON CO CATALYSTS AND NI-CO BIMETALLIC CATALYSTS. ADVISOR : ASST. PROF. SUPHOT PHATANASRI, D.ENG., 80 pp.

The cobalt catalysts (cobalt content by weight: 7%, 10% and 15%) and cobalt-nickel bimetallic catalysts (cobalt-nickel content by weight: 3.5%-3.5%, 5%-5%, 7%-7%, 10%-10% and 15%-15%) were studied in dry reforming of methane for hydrogen and synthesis gas production. All catalysts were synthesized by the wetness impregnation method. The dry reforming of methane was carried out at 700^{o}C, atmosphere pressure using a mixture; CH_4 and CO_2 in ratio 1:1. It was found that, after 120 minutes, the catalysts that gave the best methane conversion are 10%Co/Al_2O_3 (61.86%) for mono-metallic catalysts and 10%Ni-10%Co/Al_2O_3 (96.86%) for bimetallic catalysts. Moreover, the effect of adding potassium promoter to 10%Ni-10%Co/Al_2O_3 catalyst was studied. The methane conversion of potassium promoted 10%Ni-10%Co/Al_2O_3 catalyst was slightly lower than one without potassium. However, the adding of promoter could significantly decrease the carbon content on the catalysts.

Department : Chemical Engineering Student's Signature .....
Field of Study : Chemical Engineering Advisor's Signature .....
Academic Year : 2013

ACKNOWLEDGEMENTS

The author would like to express her greatest thankfulness and appreciation to her adviser, Assistant Professor Dr. Suphot Phatanasri for his instruction and valuable suggestions throughout this study. Without his guidance and persistent help this thesis would not have been possible.

Most of all, the author would like to thanks her parents for their endless love and support. Moreover, the author wishes to thanks all my friends and members of the center of Excellent on Catalysis & Catalytic Reaction Engineering, Department of Chemical Engineering, Chulalongkorn University for their assistance and friendly encouragement. And she also very thanks for special suggestion to Miss Nuchchanok Yoonpan who helped to training and consulting in this work.

CONTENTS

Page

Page

Page

LIST OF TABLES

LIST OF FIGURES

Figure Page

CHAPTER I
INTRODUCTION

1.1 Background

Nowadays world population is growing steadily and expected to increase by 36% to 8.9 billion people around the world in 2050. Consequence, to the main energy use will increase by 77%.However, source of energy in the present are unsustainable fossil fuels **[1]** or referred as hydrocarbon compounds such as coal, crude oil and natural gas which come from the transformation of plant and animal remains in the deposition of the lithosphere under appropriate temperature and pressure. Therefore, we should search the other renewable energy sources for sustainable use. A clean energy such as hydrogen can be used as a renewable alternative to conventional fuels.

A process that are widely used to synthesis hydrogen is carbon dioxide reforming of methane reaction. This process converts two greenhouse gases (CH_4 and CO_2) to valuables products **[2-5]**, hydrogen and also can to produce carbon monoxide. The hydrogen is used as a fuel cell, in the synthesis of ammonia and hydrogenation reaction. In addition, the mixture of hydrogen and carbon monoxide, celled synthesis gas can be used as a raw material in the production of methanol and dimethyl ether and used in Fischer-Tropsch synthesis **[6]**.

The CO_2 reforming of CH_4 is endothermic reaction that required high temperature condition for better conversion. The high temperature reaction results in deactivation by carbon deposition on catalysts and/or sintering of metallic particles during the reaction **[7-13]**. Hence, catalysts should have high thermal stability. Commonly, the supported metal catalysts are transition metal group VIIIB such as ruthenium, cobalt, nickel, rhodium, palladium, iridium and platinum **[14]**. Although noble metal catalysts group (palladium, platinum, rhodium, ruthenium and iridium) give more active and less deactivation, their high cost and non-availability make them not suitable for industrial use **[15-16]**. The alternative is to develop the high active and less

deactivation catalysts from non-noble metal catalysts group, such as nickel and cobalt **[17]**.

In this research, we investigate the effect of using the Co/Al_2O_3 catalysts, Ni-Co/Al_2O_3 bimetallic catalysts and addition the potassium promoter into catalyst for the carbon dioxide reforming of methane reaction to obtain high conversion and low coke deposits. We also characterized the catalysts using XRD, BET, TGA, SEM, XPS, and NH_3-TPD techniques.

1.2 Objectives

1.2.1 To determine the optimum of cobalt and nickel-cobalt content on the catalysts to obtain high activity and stability on the carbon dioxide reforming of methane catalysts.

1.2.2 To study the effects of cobalt monometallic and nickel-cobalt bimetallic catalysts properties and catalysts performance on the carbon dioxide reforming of methane reaction.

1.2.3 Investigate the effect of potassium promoter in the catalytic properties on carbon dioxide reforming of methane reaction.

1.3 Scopes of the research

1.3.1 Preparation of Al_2O_3 by sol-gel method as support and loading active metal were prepared by impregnation method.

1.3.2 Investigation for catalytic performance of cobalt over alumina$_{(sol\text{-}gel)}$ supported catalysts and nickel-cobalt over alumina$_{(sol\text{-}gel)}$ supported bimetallic catalysts in the carbon dioxide reforming of methane reaction under the following condition:

- Reaction temperature 700^{o}C.
- Atmospheric pressure.
- The mixture reactant gas consisted of methane and carbon dioxide, mixed at molar ratio of 1. The feed flow rate of 125 ml/min
- The composition of reactants and products was analyzed by thermal conductivity detector type gas chromatograph.

1.3.3 Characterization of all catalysts by using various techniques:

- X-ray diffraction (XRD) patterns to study the crystallite phase.
- Nitrogen adsorption to determine the specific surface area.
- Thermogravimetric analysis (TGA) to study carbon deposition.
- Scanning electron microscopy (SEM) to study the morphology of carbon deposition on spent catalysts, the metal particle size and metal distribution of the catalysts.
- X-ray photoelectron spectroscopy (XPS) to determine the amount of element on the surface catalysts.
- Ammonia temperature program desorption (NH_3-TPD) to determine acidity of catalysts.

1.4 Research methodology

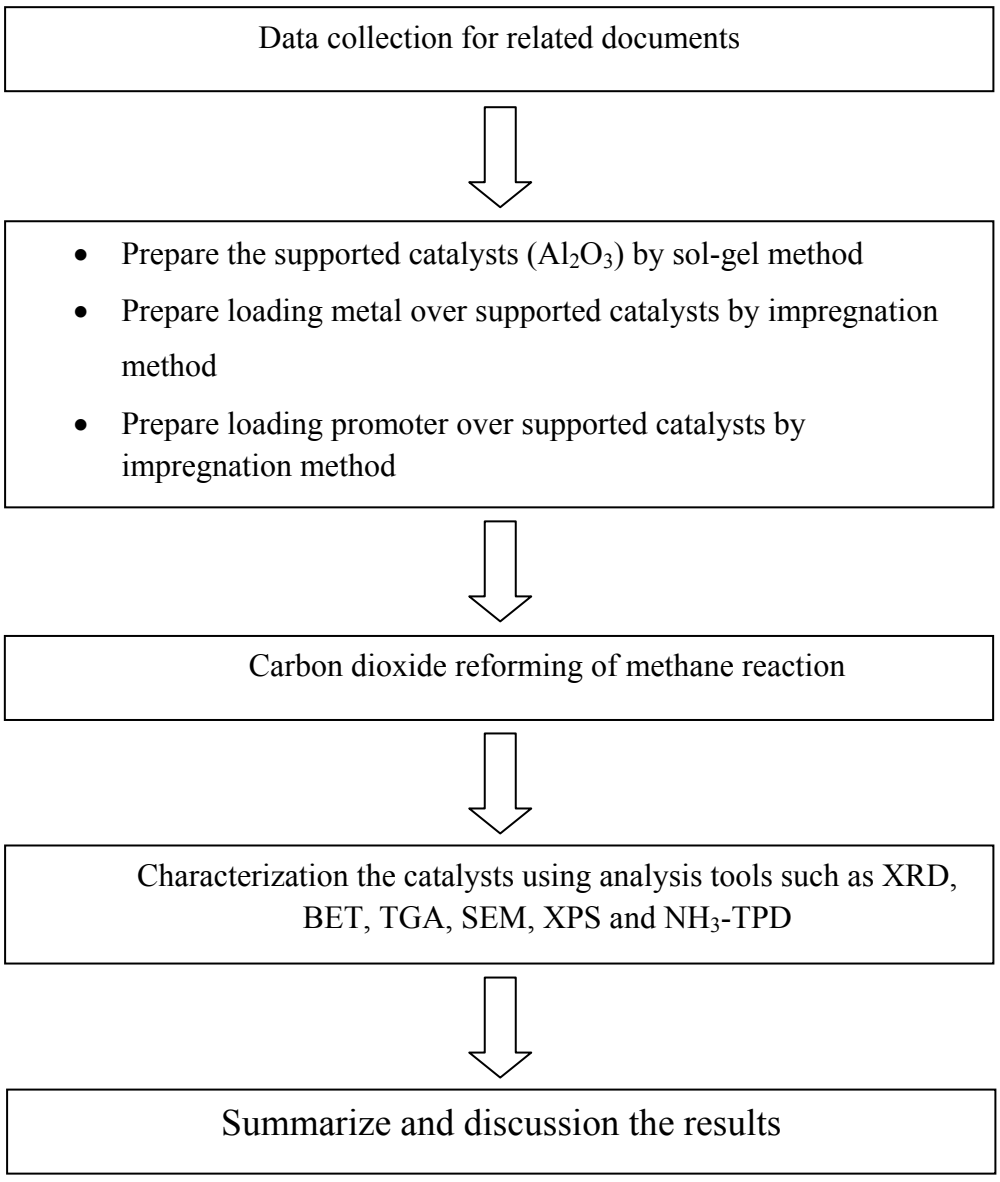

CHAPTER II
THEORY

2.1 Production of hydrogen

The production of hydrogen fuel can be produced many processes. However, the process is studied most commonly is reforming reaction because expected to developed into a commercial process. The reforming can be divided to several categories depend on type of reactant used as follows:

1) Steam reforming is an effective process to produce hydrogen that low cost. Making it is used commercially. The principle of process is entering the steam in system to react with hydrocarbons compound at a gas phase such as natural gas and biogas, etc. The hydrogen is extracted from water and hydrocarbon, the remaining oxygen from the water, hydrocarbons compound and carbon residue combination as carbon monoxide.

$$CH_4 + H_2O \rightarrow CO + 3H_2 \qquad \Delta H^o_{298} = 206.3 \text{ kJ/mol}$$

2) Carbon dioxide reforming or dry reforming is similar to the steam reforming but, this process will use of carbon dioxide as a reactant. The advantage is to reduce carbon dioxide which is a greenhouse gas in the atmosphere. It is also easier to control than the steam reforming. However the catalyst may deactivate rapidly due to the surface of catalyst is covered by the carbon.

$$CH_4 + CO_2 \rightarrow 2CO + 2H_2 \qquad \Delta H^o_{298} = 247.3 \text{ kJ/mol}$$

3) The partial oxidation is a process between hydrocarbons and oxygen. This process have the advantage is does not require external energy input because the reaction is exothermic, resulting the generate energy in the system. But the limitations of this process, the amount of oxygen fed to the system must not too high because the rest of oxygen will react with hydrogen and convert to water. As a result, the loss of hydrogen. In addition, another important limitation of this process is in commercial operation will higher cost than the other reforming. Due to the system must be separate oxygen from air before. If you do not separate the oxygen, the concentration of hydrogen decreased.

$$CH_4 + \tfrac{1}{2}O_2 \rightarrow CO + 2H_2 \qquad \Delta H^o_{298} = -35.6 \text{ kJ/mol}$$

$$CH_4 + 2O_2 \rightarrow CO_2 + 2H_2O \qquad \Delta H^o_{298} = -880 \text{ kJ/mol}$$

Hydrogen, is regarded as an energy for combustion, high performance, clean, and environmental friendly because when burned with oxygen. The byproduct is only water vapor. Unlike from the other fuel, carbon dioxide as a byproduct, which is a greenhouse gas cause a global warming phenomenon. In addition the hydrogen can be applied benefit a lot such as a fuel cell, in the production of ammonia and hydrogenation/hydrotreating reaction.

2.2 Carbon dioxide reforming of methane

The carbon dioxide reforming of methane is a very interesting reaction. There are studies both the academic and industrial utilization, as various advantages such as: (a) reducing of carbon dioxide and methane, which are both the greenhouse gases, (b) converting of methane and carbon dioxide to hydrogen and valuable synthesis gas, (c) producing synthesis gas with a hydrogen/carbon monoxide ratio is close to 1, which is more appropriate for use in the production of oxygenated compounds and the production of liquid hydrocarbons in the Fischer-Tropsch synthesis **[3,15,18]**. The

products of this reaction, hydrogen could be applied as fuel cells and more, as mentioned above. Another product is the synthesis gas, a mixture of carbon monoxide and hydrogen can be used a raw material in the production of methanol, dimethyl ether and Fischer-Tropsch synthesis **[6]**

Table 2.1 Overall reaction for carbon dioxide reforming of methane.

(1)	$CH_4 + CO_2 \rightleftharpoons 2CO + 2H_2$	$\Delta H^o_{298} = 247.3$ kJ/mol $\Delta G^o = 61770 - 67.32T$	CO_2 reforming of CH_4
(2)	$CH_4 \rightleftharpoons C + 2H_2$	$\Delta H^o_{298} = 75$ kJ/mol $\Delta G^o = 2190 - 26.45T$	CH_4 decomposition
(3)	$2CO \rightleftharpoons CO_2 + C$	$\Delta H^o_{298} = -171$ kJ/mol $\Delta G^o = -39810 + 40.87T$	CO disproportionation or Boudouard
(4)	$CO_2 + H_2 \rightleftharpoons CO + H_2O$	$\Delta H^o_{298} = 41$ kJ/mol $\Delta G^o = -8545 + 7.84T$	Reverse water-gas shift
(5)	$CO + H_2 \rightleftharpoons C + H_2O$	$\Delta H^o_{298} = -131$ kJ/mol	Reverse carbon gasification

The reaction equilibrium for carbon dioxide reforming of methane (1), usually occur simultaneously with reverse water-gas shift reaction (4), results a H_2/CO ratio of less than unity. In addition the side reaction, CH_4 decomposition (2), and CO disproportionation or Boudouard reaction (3) were involved with carbon deposition on the surface catalyst **[19]**. The equilibrium constant of the carbon dioxide reforming

of methane reaction (1), is a strongly endothermic reaction which the conversion are increases seriously with increasing reaction temperature **[20]**. However, methane decomposition (2), and reverse water-gas shift reaction (4), which are moderately endothermic reactions. Hence, the raising in temperature increases the rate of reactions. The Boudouard reaction (3) and the reverse carbon gasification reaction (5), are exothermic reaction. Therefore, the thermodynamic does not prefer at higher temperatures. In conclusion, high temperature is more favorable for the carbon dioxide reforming of methane (1) than those of the side reactions (2, 3, and 5) **[18]**.

Because the carbon dioxide reforming of methane reaction is strongly endothermic it required high temperature. Hence, the main drawback of this reaction is rapid deactivation by carbon deposition on surface catalyst or sintering of metallic particles or metal oxidation. Thus, the selection of appropriate catalysts and supports are needed to prevent the deactivation.

2.3 Composition of catalyst

For the successful application of the carbon dioxide reforming of methane reaction, we need to consider two main factors which are cost and performance. The desired properties of catalyst are the resistance to carbon deposition and the excellence activity in the reaction. Therefore, the study in the appropriate of catalysts and supports are important to achieve the desired objectives **[21]**.

The supported metal catalysts for carbon dioxide reforming of methane are those based on transition metal group VIIIB. Particularly, noble metals group, Rh, Ru, Pd, Pt and Ir lead to excellent catalytic activity and lower carbon deposition in the reaction **[22]**. However, their high cost and limited availability, so unsuitable for industrial scale. Therefore, another metal with appropriate activity, cost and availability such as nickel and cobalt must be used.

2.3.1 Metal catalyst

Cobalt

Cobalt-based catalysts began to been widely studied for the carbon dioxide reforming of methane because had good activity, availability and low cost **[23-24]**. Moreover, cobalt also has good activity which may help to promote the carbon resistance of the catalyst **[25]**.

Many cobalt compounds are used in chemical reactions such as cobalt acetate is used for the convert of xylene to terephthalic acid, the precursor to the bulk polymerpolyethylene terephthalate. Generally catalysts are the cobalt carboxylates. They are also used in paints, varnishes, and inks as "drying agents" through the oxidation of drying oils **[26]**.

Cobalt-based catalysts are also important in reactions relate with carbon monoxide. The reforming reaction such as stream reforming and carbon dioxide reforming, useful in hydrogen production, uses cobalt oxide-base catalysts. Moreover, cobalt is also a catalyst in the Fischer–Tropsch reaction, used in the hydrogenation of carbon monoxide into liquid fuels **[27]**.

Physical Properties

From Table 2.2 shows the physical property of cobalt

Table 2.2 Physical properties of cobalt **[28]**

Parameters	**Value**
Name	Cobalt
Symbol	Co
Atomic number	27
Element category	transition metal
Atomic weight	58.93
Electronegativity	1.88 (Pauling scale)
Ionization energies, $kJ \cdot mol^{-1}$	
• 1st	760.4
• 2^{nd}	1648
• 3^{rd}	3232
Latent heat of fusion, $\Delta H_{fus} J/g^a$	395
Boiling point, ^oC	3100
Latent heat of vaporization at bp, $\Delta H_{vap} kJ/g^a$	6276
Specific heat, $J/(g \cdot {}^oC)^a$	
• 15-100^oC	0.442
• Molten metal	0.560
Coefficient of thermalexperature, $^oC^{-1}$	
• cph at room temperature	12.5
• fcc at 417^oC	14.2

Table 2.2 Physical properties of cobalt (cont.)

Parameters	**Value**
Thermal conductivity at 25°C, W/(m·K)	69.16
Thermal neutron absorption, Bohr atom	34.8
Resistivity, at 20°C[b], 10^{-8} Ω·m	6.24
Residual induction, T[c]	0.490
Coercive force, A/m	708
Young's modulus, Gpac	211
Poisson's ratio	0.32
Shear modulus, Gpa	75
Bulk modulus, Gpa	180
Mohs hardness	5.0
Vickers hardness, MPa	1043
Brinell hardness, MPa	700

[a] To convert J to cal., divided by 4.184

[b] Conductivity = 27.6% of International Annealed Copper Standard

[c] To convert T to gauss, multiply by 10^4

2.3.2 Support catalyst

Alumina

Alumina, one of the most common supports due to high thermal stability, the several of physical, chemical and catalytic properties.

Alumina, the chemical formula is Al_2O_3 is found naturally in the form of the mineral corundum usually has a white or colorless. If there are impurities in the structure will cause different colors make it more beautiful and become valuable minerals such as the red of ruby caused by chromium in the structure of alumina. The alumina structures consist of aluminum and oxygen bond which very strong. Breaking the bond requires high energy. In addition alumina is good electrical insulation properties, resistant to heat and corrosive from chemicals as well. Alumina in the industry is produced from bauxite mineral by the process is called Bayer process. To eliminated impurities and changed aluminum hydroxide to aluminum. Alumina is produced mainly (over 90 percent) is used as a precursor in the production of aluminum metal. The rest (about 10 percent) to be used in the form of alumina directly.

There are many benefits of alumina. It is used as an ingredient in ceramic products. To achieve greater strength, but also can be made into useful products, such as the refractory material in furnace, crucible for the jewelry industry, spark plug for automotive industry, part of the replacement organs, et al,.

Physical Properties

The structure and properties of an alumina depend on preparation, purity, dehydration, and thermal treatment history. In addition the more acidic, high

surface area of alumina hydrate are produced at relatively low temperature by precipitation

From either acidic or basic solutions are transformed by dehydration and treatment at high temperature to transitional β, γ, η, χ, σ, and θ-alumina and ultimately α-alumina, all of lower surface area and acidity. Some of the more known transformations were illustrated as a function of calcination temperature in Figure 2.1, and the physical and structural characteristics of significant alumina phase formed at different calcinations temperatures were listed in Table 2.3.

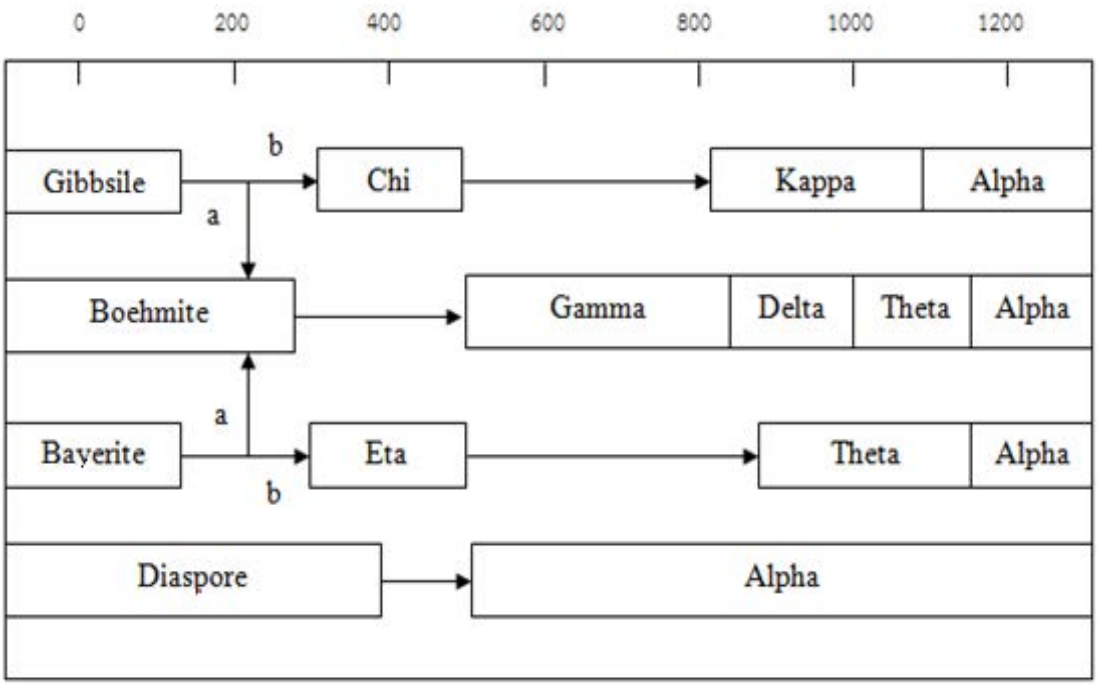

Figure 2.1 Thermal transformation sequence of the aluminum hydroxide **[29]**.

Table 2.3 Physical and structural characteristic of common aluminum oxides **[30]**.

T_{calc}(^{o}C)	Alumina phase	SA, (m^2/g)	V_{pore},(cm^3/g)	D_{pore}, (nm)
250	pseudoboehmite	390	0.50	5.2
450	γ-alumina	335	0.53	6.4
650		226	0.55	9.8
850		167	0.58	14
950	δ-alumina	120	0.50	16.6
1050	θ-alumina	50	0.50	28
1200	α-alumina	1-5		

Synthesis

The synthesis of alumina can be done in several methods like solvothermal method and sol-gel method. For this research has investigated the influences of alumina was prepared by sol-gel method.

The sol–gel method show to be promising as low cost, offers good adhesion to metallic surface with chemical bonding, and easy adaptability in industries because simple application procedure. The main advantage of sol–gel method is capacity to yield coatings with a various range of compositions on different substrates regardless of size or geometry of the work **[31]**.

2.3.3 Promoter

Promoter is a substance added to a catalyst in order to improve its performance in a chemical reaction. Promoter can be divided into various types.

1) Textural promoters help increasing the stability of the structure of a catalyst but do not increase the reactivity of the catalyst. For example, the addition of alumina, silica or other relatively inert substance that inhibits the sintering of metal.

2) Chemical promoters are additives those improve the activity and selectivity of the catalytic phase. They provide electron exchanger on the surface of the catalysts. Normally, chemical promoters include alkali, alkaline earth and halogen group.

However, there are other promoters that can enhance the performance of catalysts but do not change the structure, electrical property or chemical property such as the promoter that can break the side reaction **[32]**.

CHAPTER III
LITERATURE REVIEWS

Factors influence the performance of catalysts used in carbon dioxide reforming of methane reaction are discussed here in this chapter. These factors include type of metal, support, and effect of bimetallic catalysts.

3.1 Metal

The catalysts for CO_2 reforming of CH_4 can be divided into two groups: (a) noble metal group catalysts such as palladium, platinum, rhodium, ruthenium and iridium. Which shown excellent catalytic performances **[33-34]**. But, these catalysts group are the cost and limited availability therefore not suitable for using industrial scale. Another group, (b) non-noble metal group catalysts such as nickel and cobalt also attention in the present and commonly studied due to low cost.

D. San Jose-Alonso and others studied metal content of Co and Ni over alumina supported catalysts (4.0, 2.5 and 1.0 wt% nominal metal content. The reaction temperature is 973 K. The results show that the amount of carbon formed is lower than that obtained with the Co and Ni reference catalysts (9 wt.%), but the CH_4 and CO_2 conversions are also lower. The 1.0 wt.% Ni and 2.5 wt.% Co catalysts show a high activity for methane conversion, an excellent stability and a very low carbon deposition **[35]**. However in the previous researched found that the nickel catalysts can be easily induce deactivation from carbon deposition **[36]**. Therefore, the cobalt catalysts have been a new choice of attention for CO_2 reforming of CH_4 reaction.

K. Takanabe and others studied the effect of reduction temperature on the catalytic behavior of 10 wt.% Co/TiO_2 catalysts in CO_2 reforming of methane to synthesis gas production. The results shown that the Co/TiO_2-anatase catalysts reduced at lower temperatures ($\leq$1073 K) had stable activities. On the contrary, the

catalyst reduced at higher temperatures (≥1123 K), that the crystal phase of TiO_2 is converted from anatase to rutile, cause almost no activity. Moreover, it was also not found the carbon deposition for any of the Co/TiO_2 catalysts **[37]**.

E. Ruckenstein and others studied the reaction behavior and carbon deposition during the dry reforming reaction on Co over the γ-Al_2O_3 supported catalysts with varied Co content loading (between 2 and 20 wt.%) and calcination temperature (between T_c=500 and 1000^oC). The results found that the stability of Co/γ-Al_2O_3 catalysts was strongly dependent on the calcinations temperature and Co content loading. The stable activities have been shown at 6wt.% Co/γ-Al_2O_3, T_c=500^oC and 9wt.% Co/γ-Al_2O_3, T_c=1000^oC. However, over the catalysts with high Co loadings (>12 wt.%), remarkable amounts of carbon were deposited during reaction, and deactivation was occurred. Moreover, the 2 wt.% Co/γ-Al_2O_3 also found serious deactivation, caused by both the carbon deposition for T_c=500^oC or the oxidation of metallic sites for T_c=1000^oC. Therefore, the mechanisms of deactivation have two different, carbon deposition and oxidation of metallic sites **[38]**.

3.2 Supported

The proper support is important in CO_2 reforming of CH_4, because it can increase the activity and also reduce carbon formation on the catalyst. Many studies have reported the results obtained from the use a various support **[12, 39-40]**. The Al_2O_3 support is one of the most commonly used because often good performance and stable.

M. Nagai and others studied the effects of the catalyst pretreatment, the ratio of CH_4/CO_2 and the CeO_2 support the on carbon dioxide reforming of methane on the Rh/Al_2O_3 catalyst using a flow micro-reactor. The oxidized or reduced Rh/Al_2O_3 catalyst had a better activity and the addition of CO_2 enhanced formation of H_2 during

the CH_4 reforming reaction furthermore, also, decreased the catalysts deactivation due to carbon deposition on the surface catalysts. The Rh/CeO_2 catalyst was less active during the reaction with CO_2 addition than the Rh/Al_2O_3 catalyst **[41]**.

H.Y. Wang and others studied the carbon dioxide reforming of methane reaction using Rh (0.5 wt.%) catalysts over the reduced supported. Two groups of oxides, reducible (CeO_2, Nb_2O_5, Ta_2O_5, TiO_2, and ZrO_2) and no reducible (γ-Al_2O_3, La_2O_3, MgO, SiO_2, and Y_2O_3) were used as supports. The no reducible metal oxides, γ-Al_2O_3, La_2O_3 and MgO gave stable activities during reaction, and the activity increased in sequence: $La_2O_3<MgO\approx\gamma$-Al_2O_3. The stable activity could was described as the strong interactions between Rh_2O_3 and support. The reducible oxides, Nb_2O_5 gave a low activity, ZrO_2 and CeO_2 showed a very long activation period, but deactivation occurred over Ta_2O_5 and TiO_2. Hence, the reducible oxide supported group gave lower yields of CO and H_2 than the no reducible oxide supported group. Conclude, MgO and γ-Al_2O_3 were the most ability supported because they gave a stable and good activity **[42]**.

L. Ji and others studied three cobalt-based catalysts with 10 wt% cobalt were prepared by conventional impregnation of commercial γ-Al_2O_3 support ($CoAl_{CO\text{-}IM}$), sol–gel made γ-Al_2O_3 ($CoAl_{SG\text{-}IM}$) and direct sol–gel processing from organometallic compounds ($CoAl_{SG}$), respectively. The results showed all three catalysts had the same activity at 750 ^oC. But, $CoAl_{SG}$ catalyst showed low catalytic activity with low reaction temperatures (550–650^oC), because of the formation of $CoAl_2O_4$. Nevertheless it had the best carbon resistivity. Rapid and large carbon deposition occurred on $CoAl_{CO\text{-}IM}$ catalyst. Compared with the $CoAl_{CO\text{-}IM}$ catalyst, the $CoAl_{SG}$ catalyst had smaller metallic Co particles, more surface OH^- species and stronger metal-support interaction. Which all these properties may useful for resistant of carbon formation **[43]**.

3.3 Prometer

N. Wang and others found that adding Mn remarkably enhanced the catalytic activity and stability of the Co–Ce–Zr–Ox catalyst prepared by the co-precipitation method. Various physico-chemical characterization techniques such as X-ray diffraction (XRD), temperature programmed reduction (TPR), O_2 temperature programmed desorption (O_2-TPD), X-ray photoelectron spectroscopy (XPS) and temperature programmed hydrogenation (TPH) were studied. The highest catalytic activity and long-term was achieved when the molar ratio of Mn/(Ce + Zr + Mn) was 10%. The surface oxygen species and oxygen mobility played important roles on the catalytic behavior. The result of TPH characterization showed that the surface coke species could be easily oxidized into CO_x for the Mn-doped nano cobalt-composite catalyst due to the higher amount of mobile oxygen. The Mn incorporation promoted the dispersion of the nano-sized CoO_x crystallites. In comparison with the impregnated samples, CoO_x species dispersed better in the co-precipitated catalysts **[44]**.

M.C. Roman-Martinez and others investigated K and Sr promoted Co alumina supported catalysts for the CO_2 reforming of methane (at 973K, CH_4:CO_2 ratio = 1:1). The catalysts have been prepared by the co-impregnation and successive impregnation methods. The characterization techniques were Atomic Absorption Spectroscopy (ICP-OES), Transmission Electron Microscopy (TEM), Energy Dispersive X-ray (EDX) and Temperature Programmed Oxidation (TPO). It was found that K is a more effective promoter than Sr. The preparation method does not affect the catalyst performance. As a result, the co-impregnation method which was the simplest had been selected to prepare K promoted catalysts. Found from the results that the amount of potassium influences both, the methane conversion and the amount of deposited carbon. The optimum amount of potassium seems to be around 0.6 wt.%, as the catalyst with this K loading presents a relatively high methane conversion (60%) and a quite low amount of deposited carbon (0.08% molar of the converted carbon) after 6 hour of reaction **[45]**.

A.E. Castro Luna and Maria E. Iriarte investigated the influence of K, Sn, Mn and Ca on modified Ni-Al_2O_3 catalyst. The modified Ni-Al_2O_3 catalyst was prepared by a sol–gel method. Catalytic activity and its resistance to coking were measured. The unmodified catalyst showed its effectiveness in the dry reforming reaction of methane with low carbon deposition and high and constant catalytic activity during over 30 hour of operation. The introduction of 0.5 wt.% of K showed constant but slightly less activity and a lower carbon deposition after the same operation period. In the case of Ca, Mn and Sn, a dramatic reduction of catalytic activity and a significant increase in carbon deposition were observed during the same period of time **[46]**.

B. Mallanna and others investigated the effect of K on the activity and stability of Ni–MgO–ZrO_2 catalysts for the dry reforming of methane. 0.5 wt.% potassium was added to 8 wt.% Ni supported MgO–ZrO_2 catalyst prepared by co-precipitation. It was found that the addition of improved both the activity and stability of this material for the dry reforming of methane. Increasing the content of potassium caused a decrease in the catalytic activity but the stabilities of the resultant catalysts were still higher than those for the un-doped catalyst. Also, the BET surface areas of the catalysts increased with an increasing potassium content **[47]**.

3.4 Bimetallic catalysts

J. Juan-Juan and others studied the Ni, Co and Ni-Co alumina supported catalysts (with 9 wt.% nominal metal content) for dry reforming of methane. The result showed that the catalysts with the highest cobalt content, Co(9) and NiCo(1-8) catalysts are the most active and stable, but produced a large amount of carbon. The higher activity showed by cobalt rich catalysts is related with the higher activity of this metal for methane decomposition reaction, which is the rate limiting step of overall reaction. Moreover, the stability of cobalt rich catalysts also related with the appeared of large particles involved in long term conversion, due to they produce non-deactivating carbon **[48]**.

K. Nagaoka and others studied cobalt and nickel bimetallic catalysts over titania-supported for carbon dioxide reforming of methane to synthesis gas production at 1023 K under ambient pressure. The results found that the bimetallic Co–Ni/TiO_2 catalysts with an appropriate Co/Ni ratio showed excellent stable activities with no carbon deposition. But the monometallic Co/TiO_2 catalyst occurred deactivation rapidly due to the oxidation of metal. However, the 10 mol% substitution of nickel in cobalt inhibited the oxidation of metal, giving a high stability. The bimetallic catalysts have advantages are good resistance to metal oxidation and coke formation **[49]**.

J. Zhang and others studied the Ni-Co bimetallic catalyst, Ni-Co-Al-Mg-O prepared using co-precipitation method for carbon dioxide reforming of methane that interests on the effects of Ni-Co content of the catalyst, and prevent the carbon formation on the surface catalyst. The metal loadings in range 1.83-14.5 wt.% of nickel and 2.76-12.9 wt.% of cobalt were used. The results found that catalysts with lower Ni-Co content (1.83–3.61 wt.% for Ni and 2.76–4.53 wt.% for Co) had higher and more stable catalytic performance with non-deactivation. In addition those catalysts also have larger surface area and better metal dispersion cause to better performance. On the other hand, the catalysts with higher Ni-Co content (5.28–14.5 wt.% for Ni and 7.95–12.9 wt.% for Co) had noticeable deactivation with carbon formation in 250 h on time **[50]**.

CHAPTER IV
EXPERIMENT

For this chapter consists of 3 sections. First, preparation process of catalysts: alumina supported by sol-gel method and cobalt active site by impregnation method. Second, the characterization of catalysts by x-ray diffraction (XRD), nitrogen physisorption, Thermogravimetric analysis (TGA), Scanning electron microscopy (SEM), X-ray photoelectron spectroscopy (XPS) and ammonia temperature program desorption (NH_3-TPD). Finally section, the studied in carbon dioxide reforming of methane reaction.

In this research, we determined the optimum metal contents and also studied the effects of adding the potassium into catalyst on catalytic performance and carbon formation.

4.1 Catalyst Preparation

4.1.1 Alumina supported by sol-gel method

Chemicals

1) Alumina Isopropoxide : AIP, $[(CH_3)_2CHO]_3Al$ from Aldrich
2) Ethanol, (C_2H_5OH) from Merck
3) Hydrochloric acid, (HCl) from Merck

Preparation of alumina supports by sol-gel method

The precursor, alumina isopropoxide dissolved in mixture of ethanol and deionized water with volume ratio 1:1 under mild stirring at 70^{o}C for 1 hr. Then hydrochloric acid was dropped into the solutions unit pH value was equal to 2.5 and

aged with stirring at 70°C about 5 hr unit eliminating the solvent. And then the alumina supported were dried at 100°C overnight and calcined under air at 550°C for 2 hr.

4.1.2 Cobalt-base metal catalyst

Chemical

1) Cobalt nitrate hexahydrate, [$Co(NO_3)_2 \cdot 6H_2O$] from Carlo Erba

Preparation of cobalt metal loading on alumina supported by impregnation method

The cobalt catalysts with various metal content (7wt.%Co, 10wt.%Co, 15wt.%Co) were prepared by the co-impregnation method using a $alumina_{(sol\text{-}gel)}$ supported and aqueous solution of $Co(NO_3)_2 \cdot 6H_2O$ of the appropriate concentration to have the metal loading above. The impregnated support was kept at room temperature for 4 hr to assure adequate distribution of metal complete. Then, the catalysts were dried at 100°C overnight and calcined under air at 500°C for 2 hr.

4.1.3 Bimetallic catalysts

Chemicals

1) Cobalt nitrate hexahydrate, [$Co(NO_3)_2 \cdot 6H_2O$] from Carlo Erba
2) Nickel nitrate hexahydrate, [$Ni(NO_3)_2 \cdot 6H_2O$] from Merck

Preparation of Ni-Co bimetallic catalysts loading on alumina supported by co-impregnation method

The bimetallic Ni-Co catalysts, with various compositions (3.5wt.%Ni-3.5wt.%Co, 5wt.%Ni-5wt.%Co, 7wt.%Ni-7wt.%Co, 10wt.%Ni-10wt.%Co and 15wt.%Ni-15wt.%Co) were prepared by the co-impregnation method using a alumina$_{(sol\text{-}gel)}$ supported and aqueous solution of $Co(NO_3)_2.6H_2O$ and $Ni(NO_3)_2.6H_2O$ of the appropriate concentration to have the metal loading above. The impregnated support was kept at room temperature for 4 hr to assure adequate distribution of metal complete. Then, the catalysts were dried at 100^oC overnight and calcined under air at 500^oC for 2 hr.

4.1.4 Adding the promoter

Chemicals

1) Cobalt nitrate hexahydrate, [$Co(NO_3)_2{\cdot}6H_2O$] from Carlo Erba
2) Nickel nitrate hexahydrate, [$Ni(NO_3)_2{\cdot}6H_2O$] from Merck
3) Potassium Nitrate, KNO_3 from BDH

Preparation of adding the potassium into the 10%Ni-10%Co bimetallic catalysts loading on alumina supported by co-impregnation method

Potassium promoted the bimetallic 10%Ni-10%Co catalysts (with nominal composition 0.1wt.%K and 1wt.%K) have been prepared by co-impregnation method using a alumina$_{(sol\text{-}gel)}$ supported and aqueous solutions of the $Co(NO_3)_2.6H_2O$, $Ni(NO_3)_2.6H_2O$ and KNO_3 of the appropriate concentration to have the metal loading above. The impregnated support was kept at room temperature for 4 hr to assure adequate distribution of metal complete. Then, the catalysts were dried at 100^oC overnight and calcined under air at 500^oC for 2 hr.

4.2 Catalyst characterization

4.2.1 X-ray diffraction (XRD)

The analysis of crystalline phases was preformed by X-ray diffraction (XRD) patterns of the samples were carried on an X-ray diffractometer SIEMENS D 5000 connected to a personal computer with Diffract AT version 3.3 program for fully control of XRD analyzer. The XRD analysis was conducted to Cu-Kα radiation between 10^{o} and 80^{o} with a generator voltage and current of 30 kV and 30 mA, respectively. The scan step was 0.04^{o}.

4.2.2 Nitrogen physisorption

The BET surface area, pore diameter and pore volume were measured by N_2 adsorption-desorption isotherm at liquid nitrogen temperature of $-196^{o}C$ using a Micromeritics ASAP 2020 with 0.2 grams catalyst. The surface area and pore size distribution were calculated by Brunauer-Emmett-Teller (BET) and Barret-Joyner-Halenda (BLH) methods.

4.2.3 Thermogravimetric analysis (TGA)

The as-spun alumina fibers was subjected to the thermogravimetric and differential thermal analysis (Diamond Thermogravimetric and Differential Analyzer, TA Instruments SDT Q600) to determine the carbon content in the sample, as well as their thermal behaviors in the range of room temperature to $1000^{o}C$. The analysis was performed at a heating rate of $10^{o}C$ /min in 100 ml/min flow of air.

4.2.4 Scanning electron microscopy (SEM)

The morphology of the carbon deposition on spent catalysts was characterized by the JEOL JSM-35 CF model at the Scientific and Technology Research Equipment Centre, Chulalongkorn University (STREC).

4.2.5 X-ray photoelectron spectroscopy (XPS)

The amount of element on the surface catalysts were analysis by X-ray photoelectron spectroscopy (XPS) using an AMICUS spectrometer equipped with a Mg Kα X-ray radiation. For a typical analysis, the source was operated at voltage of 15 kV and current of 12 mA. The pressure in the analysis chamber was less than 10^{-5} Pa.

4.2.6 Temperature Programmed Desorption of Ammonia (NH_3-TPD)

The acid properties of prepared catalysts were observed by Temperature Programmed Adsorption of Ammonia (NH_3-TPD) equipment by using Micromeritics chemisorp 2750 Pulse Chemisorption System. In an experiment, 0.10 g of the catalyst sample was placed in a quartz tube and pretreated at 500^{o}C in a flow of helium. The sample was saturated with 15%NH_3/He. After saturation, the physisorbed ammonia was desorbed in a helium gas flow about 30 min. Then the sample was heated from 40 to 500^{o}C at a heating rate 10^{o}C/min. The amount of ammonia in effluent was measured via TCD signal as a function of temperature.

4.3 Catalytic performance test

4.3.1 Chemicals for reaction

1) UHP Nitrogen gas, 99.999%

2) UHP Hydrogen gas, 99.999%

3) Feed gas: consisted of 50% methane balance carbon dioxide (molar ratio1:1)

4.3.2 Instrument and Apparatus

(a) Reactor: The reactor was a fixed bed flow reactor made from a quartz tube length of 47 mm. and inner diameter of 12 mm.

(b) Automatic Temperature and controller: There is a magnetic switch connected to a variable voltage transformer and a temperature controller connected to a thermocouple attached to the catalyst bed in reactor. A dial setting established a set point at any temperature within the range between 0^{o}C to 1000^{o}C.

(c) Electric Furnace: This supply the required heated to the reactor for reaction. The reactor could be operating at 700^{o}C.

(d) Gas Controlling System: Gas was equipped with pressure regulator (0-120 psig), an on-off valve and needle valve were used adjust flow of gas.

(e) Gas Chromatographs: Operating conditions were shown in Table 4.1.

Table 4.1 Operating condition of gas chromatograph for CO_2 reforming of CH_4

Gas Chromatograph	**Shimazu, GC 8A**	
Detector	TCD	TCD
Column	Porapack-Q	Molecular sieve 5A
Carrier gas	Ar	Ar
Carrier gas flow	30 ml/min	30 ml/min
Column Temperature		
- Initial	60°C	60°C
- Final	60°C	60°C
Detector temperature	100°C	100°C
Injector temperature	100°C	100°C
Analyzed gas	CO_2	H_2, CH_4, CO

4.3.3 Reaction Method

The carbon dioxide reforming of methane was carried out at atmospheric pressure in fixed-bed flow reactor (quartz tube, inner diameter 12 mm and length 47 mm) packed with 0.2 g catalyst. The reactor temperature was measured and controlled by K-type thermocouple positioned at the middle of catalyst bed. The catalysts were reduced in pure hydrogen (50 ml/min) at 600°C for 1 h. Then, the hydrogen was replaced by pure nitrogen (50 ml/min) and the system was heated (10°C/min) to the reaction temperature for 45 min before. The catalytic performance test was carried out at 700°C. The feed gas consisted of methane and carbon dioxide (molar ratio 1:1), and

feed flow rate 125 ml/min. Figure 4.1 shown the scheme diagram of CO_2 reforming of CH_4 reaction.

The gas compositions of reactants and products was analyzed by thermal conductivity detector-type gas chromatograph (Shimudzu, GC-8A) equipped with a Porapak-Q and Molecular sieve 5A packed column. Argon was used as carrier gas (30 ml/min).

The conversions of CO_2 and CH_4 are defined in Equation (1) and (2) and the selectivity of H_2 and CO are defined in Equation (3) and (4), respectively

$$Equation(1): X_{CH_4} = \frac{[CH_4]_{in} - [CH_4]_{out}}{[CH_4]_{in}} \times 100$$

$$Equation(2): X_{CO_2} = \frac{[CO_2]_{in} - [CO_2]_{out}}{[CO_2]_{in}} \times 100$$

$$Equation(3): S_{H_2} = \frac{[H_2]_{out}}{[H_2]_{out} + [CO]_{out}} \times 100$$

$$Equation(4): S_{CO} = \frac{[CO]_{out}}{[H_2]_{out} + [CO]_{out}} \times 100$$

$[CH_4]_{in}$ and $[CO_2]_{in}$ are the flow rates of the reactants feed and $[CH_4]_{out}$, $[CO_2]_{out}$, $[H_2]_{out}$ and $[CO]_{out}$ are the flow rates of the corresponding gas compositions in the carbon dioxide reforming of methane reaction.

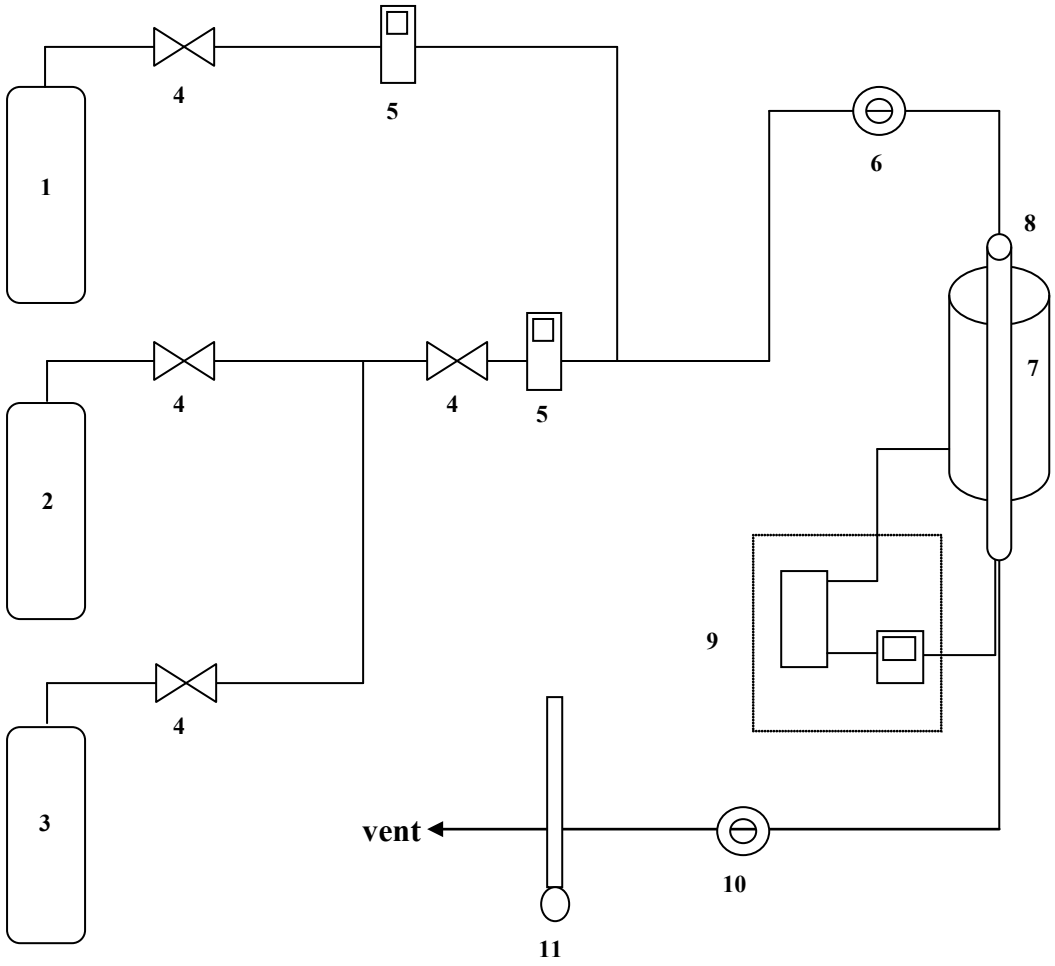

1. CH_4:CO_2 balance gas (1:1 ratio)
2. N_2 gas cylinder
3. H_2 gas cylinder
4. Ball valve
5. Mass flow controllers
6. Inlet gas injection port
7. Furnace
8. Quartz tube
9. Temperature controller and variable voltage transformer
10. Outlet gas injection port
11. Bubble flow

Figure 4.1 Diagram of CO_2 reforming of CH_4

CHAPTER V
RESULTS AND DISCUSSION

This chapter was divided into three main sections: The first section, (5.1) was the study of cobalt-monometallic catalysts. Next section, (5.2) was the study of nickel-cobalt bimetallic catalysts. And the last section, (5.3) was the study of potassium promoted 10%nickel-10%cobalt bimetallic catalysts. Each section presents the catalytic activities in carbon dioxide reforming of methane reaction and catalyst characterization by several techniques such as XRD, BET, TGA, SEM, XPS and NH_3-TPD

5.1 Effect of cobalt-monometallic over alumina$_{(sol\text{-}gel)}$ supported catalysts

5.1.1 The catalytic activities in carbon dioxide reforming of methane

This section was the study of carbon dioxide reforming of methane in order to determine the catalytic activity of the prepared catalysts were alumina$_{(sol\text{-}gel)}$ supported over cobalt base catalysts. The catalysts were reduced in H_2 at 600^{o}C for 1 h in a reactor. After, the reaction carried out at 700^{o}C, 1 atm with CH_4/CO_2 flow rate = 125 ml/min.

The CH_4 conversion of catalysts for carbon dioxide reforming of methane reaction was showed in Figure 5.1. The results showed that the 10wt.%Co/Al_2O_3 catalyst showed the highest conversion was 61.86%. The CO_2 conversion profiles were similar to those of CH_4 conversion, thus were not showed in this place.

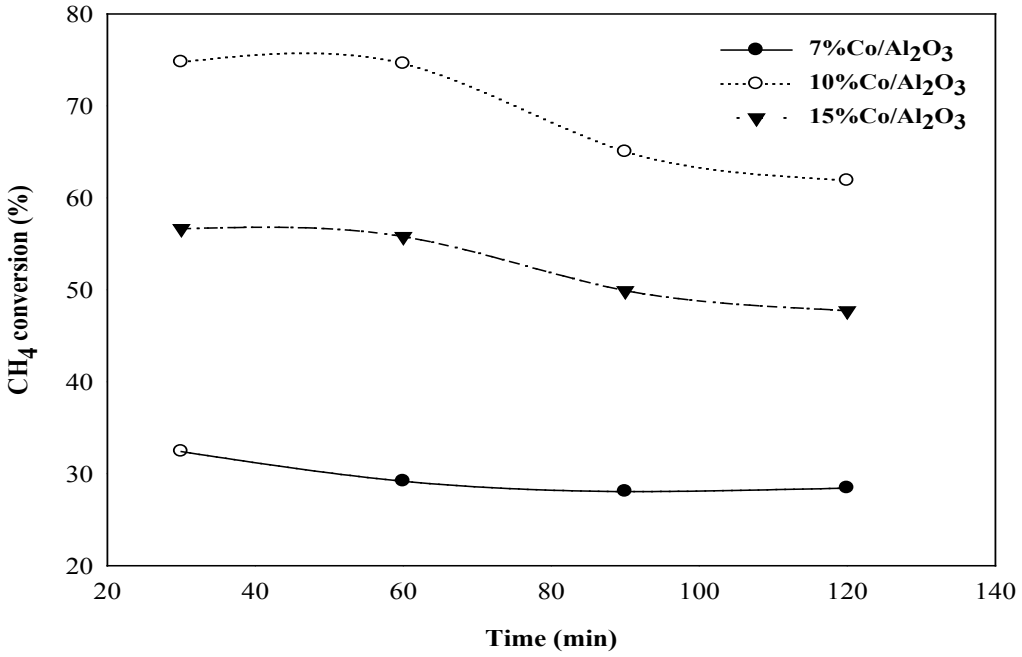

Figure 5.1 The effect of cobalt mono-metallic catalysts on the CH_4 conversion

5.1.2 Catalysts characterization

5.1.2.1 X-ray diffraction (XRD)

The crystalline phase of prepared catalysts was analyzed by X-ray diffraction (XRD). The 7wt.%Co, 10wt.%Co and 15wt.%Co were impregnated over $Al_2O_{3(sol\text{-}gel)}$ supported then, after calcinations in air at 500°C for 2 hours. These catalysts were tested by XRD that showed in Figure 5.2. The XRD characteristic peaks corresponding to Co_3O_4 were observed at $2\theta = 31^o$, 37^o, 45^o, 59^o and 65^o in all prepared cobalt-base catalysts. Moreover, at $2\theta = 46^o$ and 67^o, the diffraction peaks corresponding to γ-Al_2O_3 were found. As the cobalt content increased, the intensity of peak also increased. The 7wt.%Co/Al_2O_3 catalyst was relatively low intensity peaks. Indicated that the crystallite size of Co_3O_4 structure is smaller than the others or the amorphous cobalt oxide/cobalt aluminate ($CoAl_2O_4$) species were occurred. The

Co_3O_4 and $CoAl_2O_4$ structure are very similar therefore are indistinguishable in X-ray diffraction **[51]**.

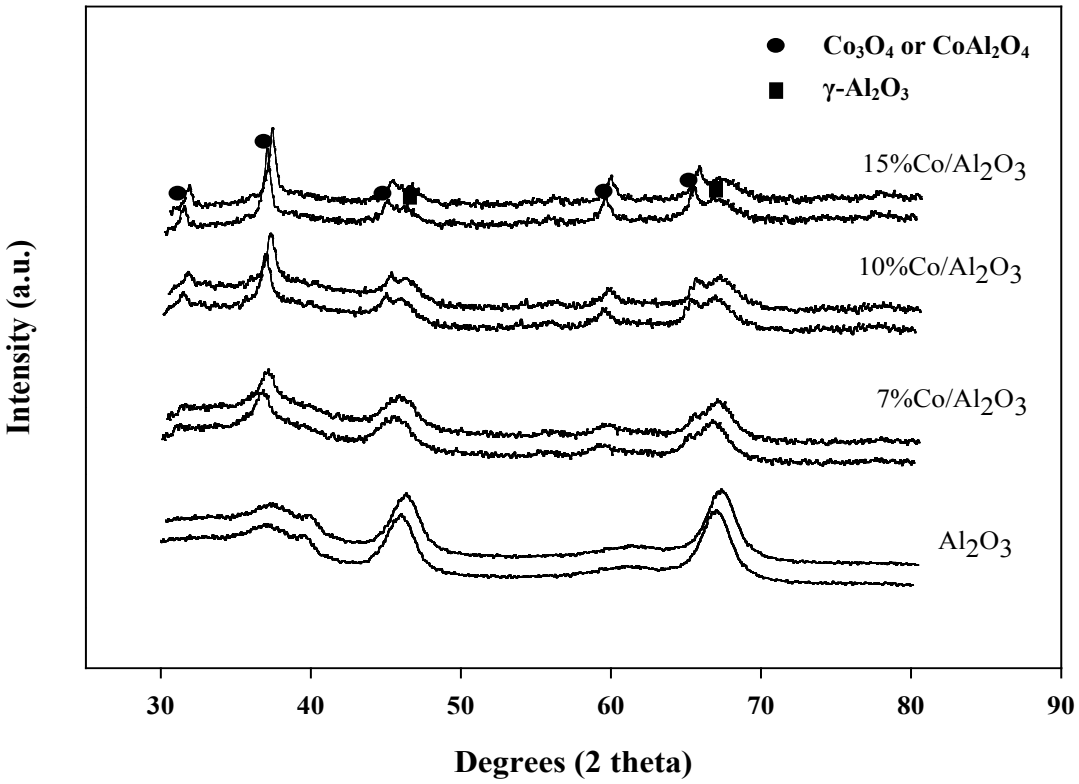

Figure 5.2 XRD patterns of the prepared Co/Al_2O_3 catalysts with various Co contents

5.1.2.2 Nitrogen physisorption

The nitrogen physisorption technique is used for determining BET surface area, pore volume and pore diameter that based on adsorption and condensation of nitrogen at liquid nitrogen temperature.

The BET surface area, pore volume and pore diameter of the prepared $Co/Al_2O_{3(sol\text{-}gel)}$ catalysts with various cobalt contents were 7wt.%, 10wt.% and 15wt.%and the $CO/Al_2O_{3(commercial)}$ with 10wt.% cobalt content were summarized in

Table 5.1. It was found that the 10%CO/$Al_2O_{3(commercial)}$ catalyst had the BET surface area was 81 m^2/g, the pore volume was 0.19 cm^3/g and the pore diameter was 5.07 nm which lower than all prepared cobalt over alumina supported obtained sol-gel method. The BET surface areas of Co/$Al_2O_{3(sol\text{-}gel)}$ catalysts were ranged between 84-117 m^2/g, the pore volume were ranged between 0.18-0.20 cm^3/g and the pore diameter were ranged between 4.81-5.21 nm. Moreover, the BET surface area, pore volume and pore diameter of all $Al_2O_{3(sol\text{-}gel)}$ supported catalysts decreased with the increasing cobalt content; 7wt.%>10wt.% >15wt.%. For 15wt.%Co/$Al_2O_{3(sol\text{-}gel)}$ catalyst showed the smallest of BET surface area, pore volume and pore diameter, it was possible that the cobalt oxide clusters block pores of alumina.

Table 5.1 The BET surface area, pore volume and pore diameter of the Co/Al_2O_3catalysts with various Co contents

Catalysts	**BET surface area (m^2/g)**	**Pore volume (cm^3/g)**	**Pore diameter (nm)**
7% Co/$Al_2O_{3(sol\text{-}gel)}$	117	0.18	4.81
10% Co/$Al_2O_{3(sol\text{-}gel)}$	104	0.20	5.21
15% Co/$Al_2O_{3(sol\text{-}gel)}$	84	0.18	5.12
10% Co/$Al_2O_{3(commercial)}$	81	0.19	5.07
$Al_2O_{3(sol\text{-}gel)}$	123	0.16	4.73

5.1.2.3 Thermogravimetric analysis (TGA)

Amount of coke was characterized by Thermogravimetric Analysis (TGA). Figure 5.3 showed the percent weight loss of spent Co/Al_2O_3 catalysts with various cobalt contents were 7wt.%, 10wt.% and 15wt.%. The results showed the few weight loss over 7wt.%Co/Al_2O_3catalyst only 6.79% decrease. However, there were

more weight loss over 10wt.%Co/Al_2O_3 and 15wt.%Co/Al_2O_3 catalyst were 11.2% and 26.94% decrease, respectively which were oxidized at about 450-570^oC. This result is consistent with previous research which found that the higher cobalt content catalyst, produce large amounts of carbon due to a larger average particle size of those catalysts **[48]**

Figure 5.4 showed DSC curves of spent Co/Al_2O_3 catalysts with various Co content. There were one endothermic peak on the DSC curves for all catalysts which presented between 440-570^oC. Expect for 15wt.%Co/Al_2O_3 catalyst also found the other endothermic peak at 610^oC. The weight loss peaks corresponded to two DSC endothermic peaks that were weight loss peaks of deposition carbon combustion on surface catalysts. There were two types of carbon, α carbon (usually occur at low temperature) which could be ridded in the reaction and β carbon (usually occur at high temperature) which could not be ridded in the reaction. Therefore, β carbon type is often the main cause of the deactivation for catalysts **[52]**.

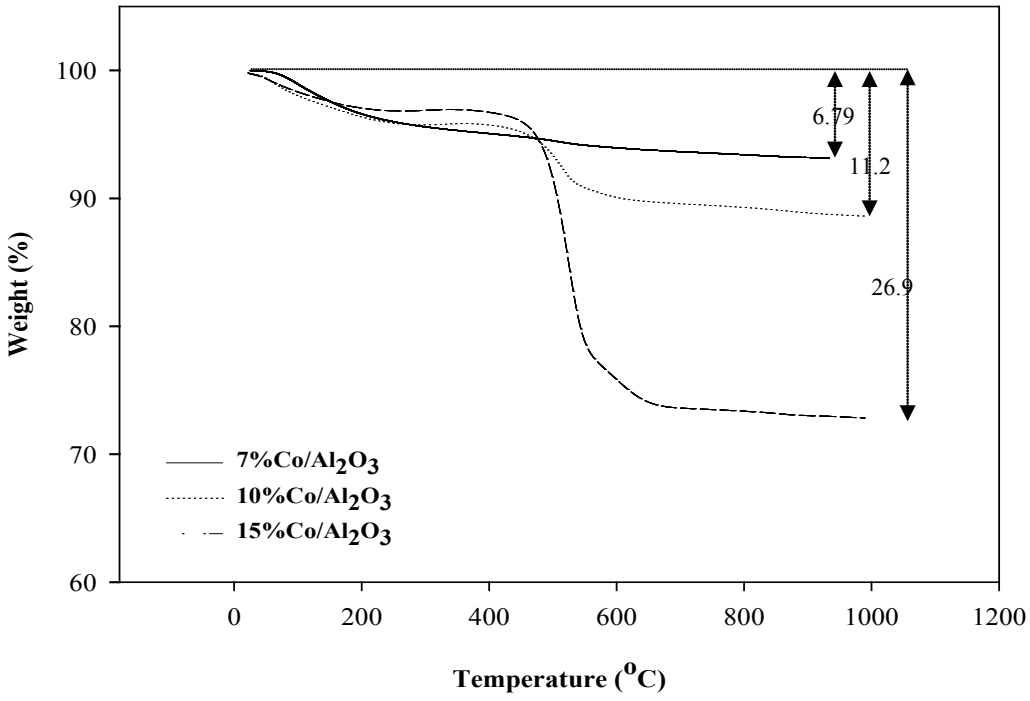

Figure 5.3 The weight loss of spent Co/Al_2O_3 catalysts with various Co contents

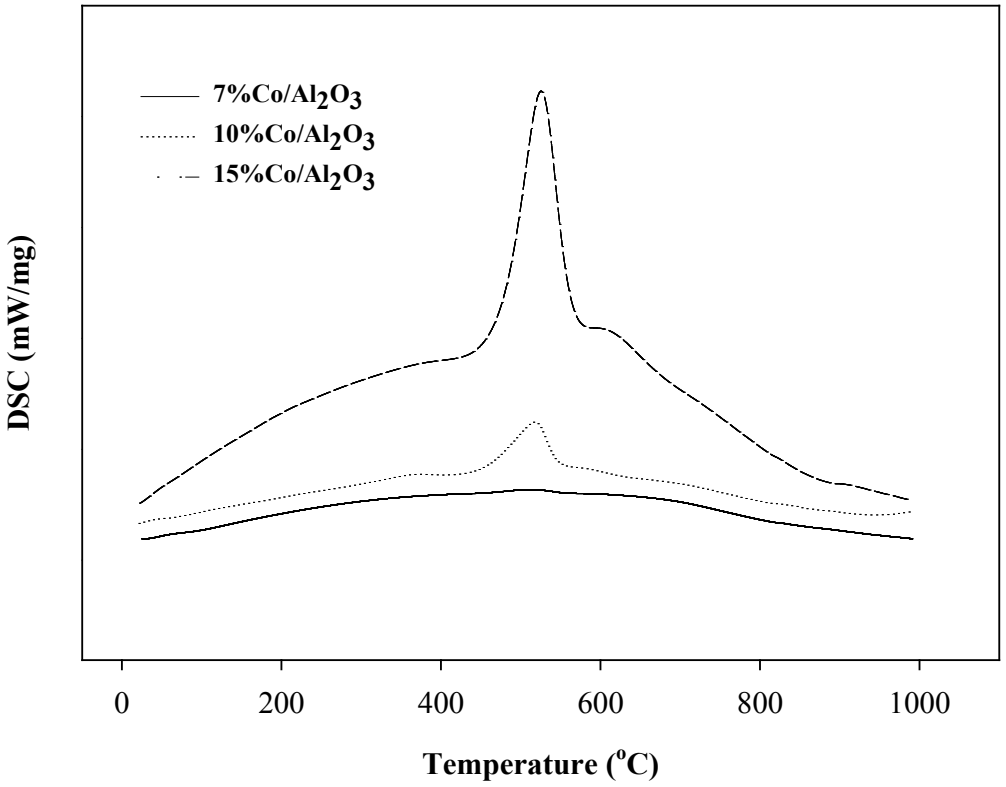

Figure 5.4 DSC curves of spent Co/Al_2O_3 catalysts with various Co contents

5.1.2.4 Scanning electron microscopy (SEM)

The morphology of the prepared Co/Al_2O_3 catalysts with various Co contents were 7wt.%, 10wt.% and 15wt.% were investigated by Scanning Electron Microscopy (SEM). Figure 5.5 showed the SEM images of fresh Co/Al_2O_3 catalysts with various Co contents before reaction. From SEM images found that all prepared catalysts had similar in particle shape and size. Figure 5.6 showed the SEM images of spent $15\%Co/Al_2O_3$ catalyst after 120 min reaction. It has been found some carbon deposit appears in a filamentous structure form

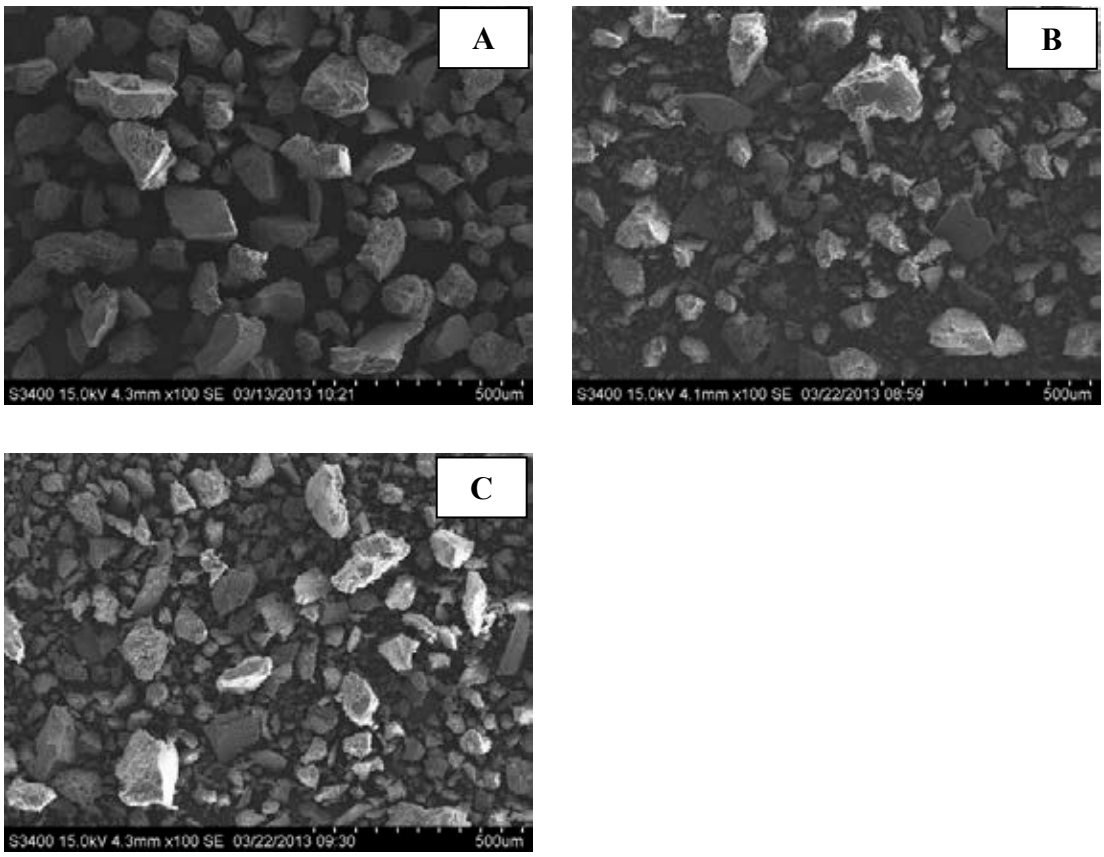

Figure 5.5 The SEM images of fresh Co/Al_2O_3 catalysts with various Co contents, (A) $7\%Co/Al_2O_3$, (B) $10\%Co/Al_2O_3$, (C) $15\%Co/Al_2O_3$

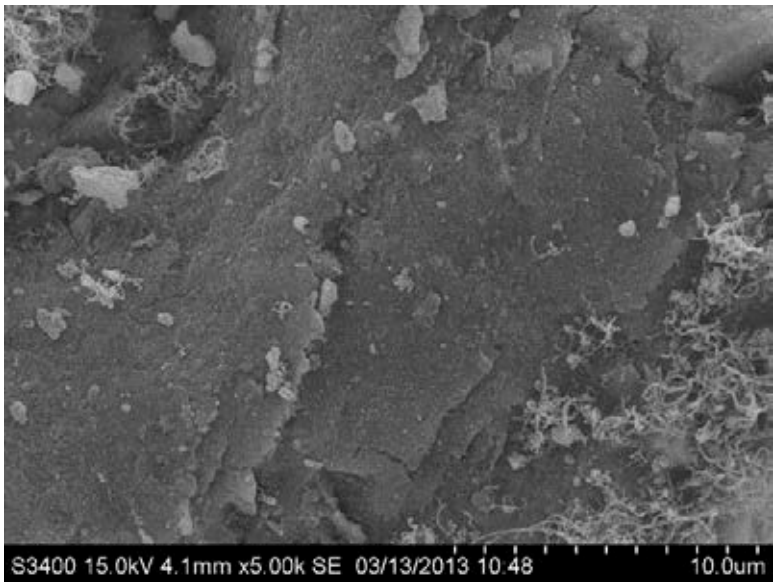

Figure 5.6 The SEM images of spent $15\%Co/Al_2O_3$ catalyst after 120 min reaction

5.1.2.5 X-ray photoelectron spectroscopy (XPS)

XPS analysis was carried out for determined the amount of elements on the surface and the interaction between metal and supports. The supported catalysts were analyzed in the Co 2p, Al 2s and O1s regarding to the binding energy regions. The binding energy of Co 2pand Al 2s and the ratio of percentages of surface atomic concentration for the prepared Co/Al_2O_3 catalysts with various Co contents were summarized in Table 5.2, indicating the binding energy of Co 2p was in the range of 781.0-781.7 eV, which all demonstration the existence of $CoAl_2O_4$. It was possible that $CoAl_2O_4$ species were formed during the process of catalyst preparation. This result was in agreement with previous research that the cobalt catalyst deactivation may come from the metal oxidation **[48]**. The binding energy of Al 2p was in the range of 73.8-75.6 eV. The ratios of atomic concentrations of catalysts could be observed that, the surface atomic concentration of Co on Al increasing with amount of Co contents.

Table 5.2 The binding energy and the ratio of percentages of surface atomic concentration for the prepared Co/Al_2O_3 catalysts with various Co contents

Catalysts	**Binding energy (eV)**		**Surface atomic concentration (%)**	
	Co 2p	**Al 2p**	**Al/O**	**Co/Al**
$7\%Co/Al_2O_3$	781.7	75.6	0.462	0.043
$10\%Co/Al_2O_3$	781.4	73.8	0.399	0.046
$15\%Co/Al_2O_3$	781	75.2	0.405	0.076
Co_3O_4**[52]**	780.0±0.7			
$CoAl_2O_4$**[52]**	781.9±0.5			

5.1.2.6 Temperature Programmed Desorption of Ammonia (NH_3-TPD)

Ammonia temperature-programmed desorption (NH_3-TPD) was a widely technique used to determine the acidity on the surface of the catalyst. The strength of the acid is related to the desorption temperature. In addition, the total amount of ammonia desorption corresponds to the amount of total acidity at surface of catalysts **[53]**.

NH_3-TPD profiles of alumina supported obtained by sol-gel method and the prepared Co/Al_2O_3 catalysts with various Co contents were 7wt.%, 10wt.% and 15wt.% are showed in Figure 5.7. From NH_3-TPD profiles, could be calculated the amount of acid sites on the surface of catalysts as showed in Table 5.3. The results found of one broad peak at low temperature in range 100-350^oC which had found involved with weak acid sites for all prepared cobalt-base catalysts. The alumina supported obtained by sol-gel method gave the highest amount of acid site which was 3.9442 mmol H^+/g. However, when loaded the cobalt metal on Al_2O_3 supported found that the acidity decreased which when the metal content increased, acidity would tends to decreased slightly. This can be explained that the acidity of the catalysts is mainly related to the surface area of γ-$Al_2O_{3(sol\text{-}gel)}$that loading the metal cobalt led to reduction of surface area, resulting in the decrease of acid sites on catalysts **[54]**.

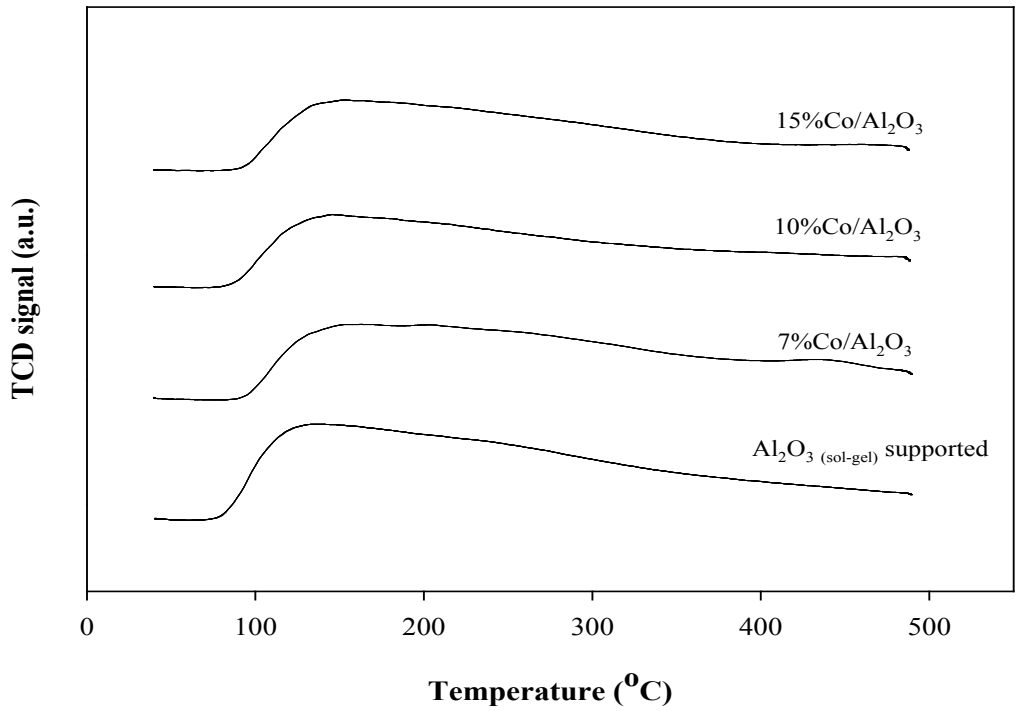

Figure 5.7 NH_3-TPD profiles of the prepared Co/Al_2O_3 catalysts with various Co contents

Table 5.3 The acidity of Al_2O_3 supported and the prepared Co/Al_2O_3 catalysts with various Co contents

Catalysts	**Total acid site, (mmol H^+/g)**
$Al_2O_{3(sol\text{-}gel)}$ supported	3.9442
7% Co/Al_2O_3	2.8713
10% Co/Al_2O_3	2.8201
15% Co/Al_2O_3	2.7016

5.2 Effect of nickel-cobalt bimetallic over alumina$_{(sol\text{-}gel)}$ supported catalysts

5.2.1 The catalytic activities in carbon dioxide reforming of methane

This section was the study of carbon dioxide reforming of methane in order to determine the catalytic activity of the prepared catalysts were alumina$_{(sol\text{-}gel)}$ supported over nickel-cobalt bimetallic catalysts. The catalysts were reduced in H_2 at 600^{o}C for 1 h in a reactor. After, the reaction carried out at 700^{o}C, 1 atm with CH_4/CO_2 flow rate = 125 ml/min.

From Figure 5.8, it can be seen that the nickel-cobalt bimetallic catalysts group showed higher CH_4 conversion than the cobalt mono-metallic catalysts group. Moreover, the catalyst that gave the highest CH_4 conversion was 10wt.%Ni-10wt.%Co/Al_2O_3, which is 96.83%.

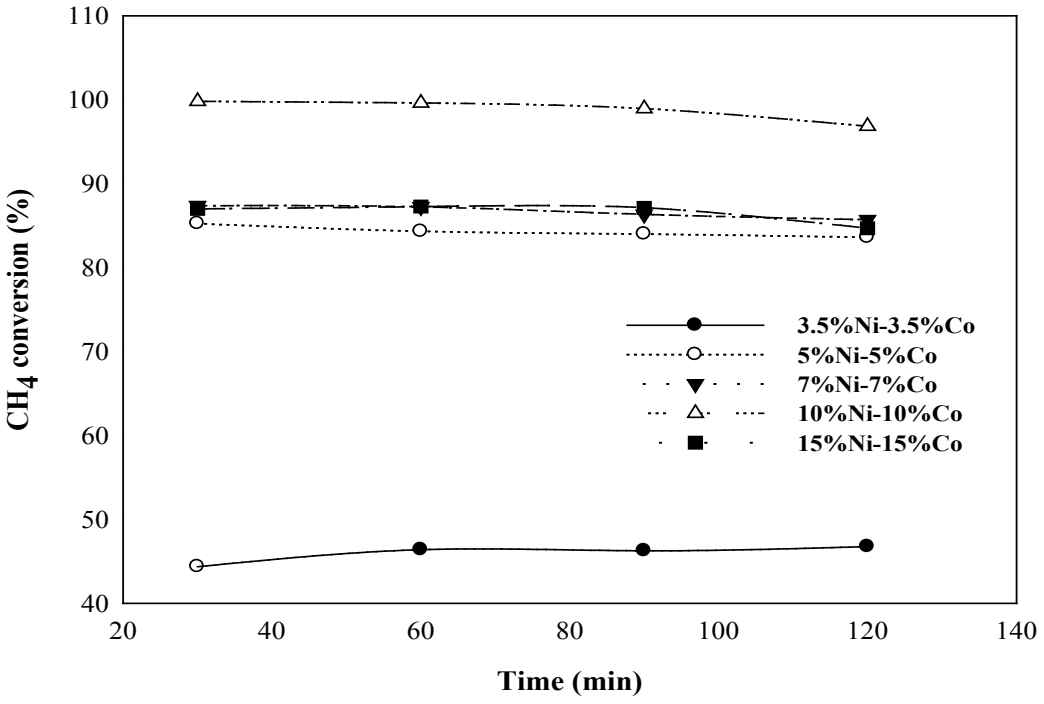

Figure 5.8 The effect of nickel-cobalt bimetallic catalysts on the CH_4 conversion

5.2.2 Catalysts characterization

5.2.2.1 X-ray diffraction (XRD)

The crystalline phase of prepared catalysts was analyzed by X-ray diffraction (XRD). The prepared Ni-Co/Al_2O_3 bimetallic catalysts with various Ni-Co contents were 3.5wt.%Ni-3.5wt.%Co, 5wt.%Ni-5wt.%Co, 7wt.%Ni–7wt.%Co, 10wt.%Ni-10wt.%Co and 15wt.%Ni-15wt.%Co were co-impregnated over $Al_2O_{3(sol-gel)}$ supported then, after calcinations in air at 500^{o}C for 2 hours. These catalysts were tested by XRD that showed in Figure 5.9. The XRD characteristic peaks corresponding to Co_3O_4 and/or NiO were observed at 2θ = 31^o, 37^o, 45^o, 59^o and 65^{o}which could not be separated by XRD because of their similar morphology. The 3.5wt.%Ni-3.5wt.%Co/Al_2O_3catalyst was relatively low intensity peaks. This result indicated that the crystallite size of Co_3O_4 and/or NiO structures is smaller than the others or the amorphous cobalt oxide/cobalt aluminate ($CoAl_2O_4$) or nickel oxide/nickel aluminate ($NiAl_2O_4$) species were occurred **[51]**. As the Ni-Co increase, the peak intensity was increasing especially at 2θ = 37^o and 65^o. In addition, the characteristic peak of NiO at 2θ = 43^o and 63^o **[55]**can also be observed for 15wt.%Ni-15wt.%Co/Al_2O_3.

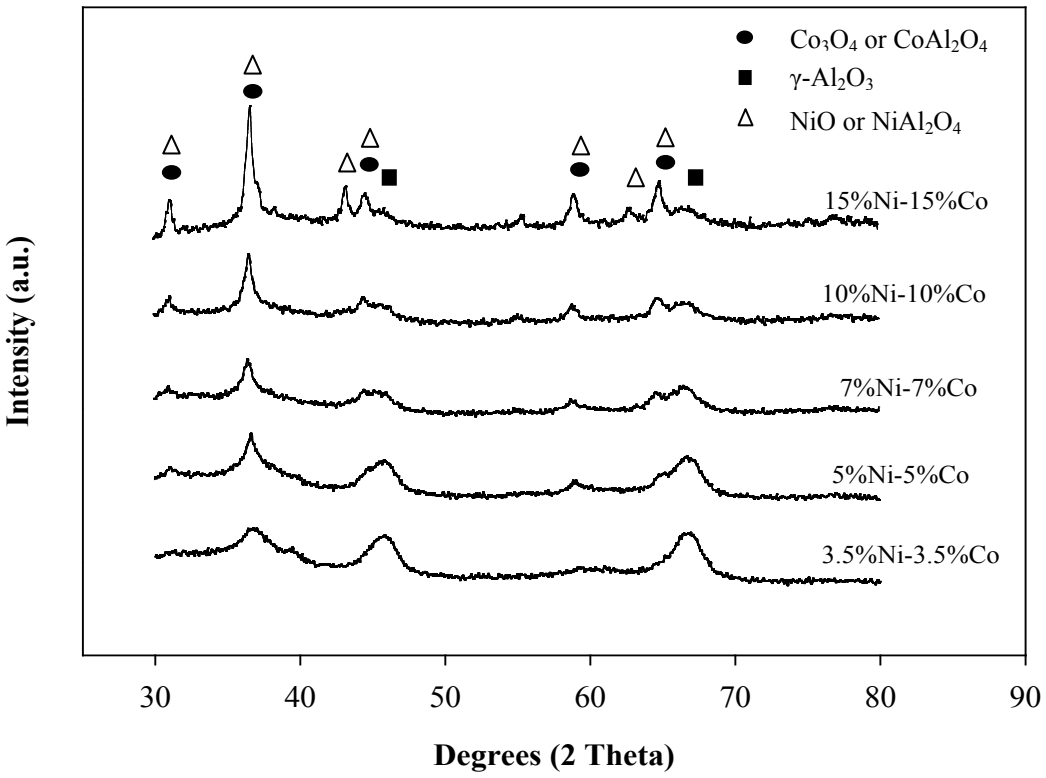

Figure 5.9 XRD patterns of the prepared Ni-Co/Al_2O_3 bimetallic catalysts with various Ni-Co contents

5.2.2.2 Nitrogen physisorption

BET surface area, pore volume and pore diameter of the prepared Ni-Co/$Al_2O_{3(sol\text{-}gel)}$ bimetallic catalysts with various nickel-cobalt contents were 3.5wt.%Ni - 3.5wt.%Co, 5wt.%Ni - 5wt.%Co, 7wt.%Ni - 7wt.%Co, 10wt.%Ni - 10wt.%Co and 15wt.%Ni - 15wt.%Co are summarized in Table 5.4. It was found that the surface areas were ranged between 86-133 m^2/g, the pore volume were ranged between 0.16-0.27 cm^3/g and the pore diameter were ranged between 5.03-5.61 nm. The BET surface are according an order of 3.5%Ni-3.5%Co>5%Ni-5%Co>7%Ni-7%Co>10%Ni-10%Co>15%Ni-15%Co, with decreased at a higher Ni-Co content.

Table 5.4 The BET surface area, pore volume and pore diameter of the Ni-Co/Al_2O_3 bimetallic catalysts.

Catalysts	BET surface area (m^2/g)	Pore volume (cm^3/g)	Pore diameter (nm)
3.5%Ni-3.5%Co/Al_2O_3	133	0.27	5.08
5%Ni-5%Co/Al_2O_3	122	0.26	5.61
7%Ni-7%Co/Al_2O_3	119	0.24	5.48
10%Ni-10%Co/Al_2O_3	114	0.21	5.10
15%Ni-15%Co/Al_2O_3	86	0.16	5.03

5.2.2.3 Thermogravimetric analysis (TGA)

Amount of coke was determined by Thermogravimetric Analysis (TGA). Figure 5.10 showed the percent weight loss of Ni-Co/Al_2O_3 bimetallic catalysts with various Ni-Co contents were 3.5wt.%Ni-3.5wt.%Co, 5wt.%Ni-5wt.%Co, 7wt.%Ni-7wt.%Co, 10wt.%Ni-10wt.%Co and 15wt.%Ni-15wt.%Co. The result showed that weight loss increased with increasing the nickel-cobalt contents. The percentage weight loss was 14.51%, 24.25%, 15.61%, 41.64% and 44.64% for 3.5wt.%Ni-3.5wt.%Co,5wt.%Ni-5wt.%Co, 7wt.%Ni-7wt.%Co, 10wt.%Ni-10wt.%Co and 15wt.%Ni-15wt.%Co catalysts, respectively. This suggests that catalysts with higher nickel-cobalt contents are appropriate in the formation of coke and led to the deactivation **[56]**.

Figure 5.11 showed DSC curves of spent Ni-Co/Al_2O_3 bimetallic catalysts with various Ni-Co contents. There was one endothermic peak on the DSC curves for all catalysts which presented between 430-570^oC. This endothermic peak associated with the type of carbon formed as described previously. The result suggested the carbon occurred in all bimetallic catalysts were corresponded to α carbon.

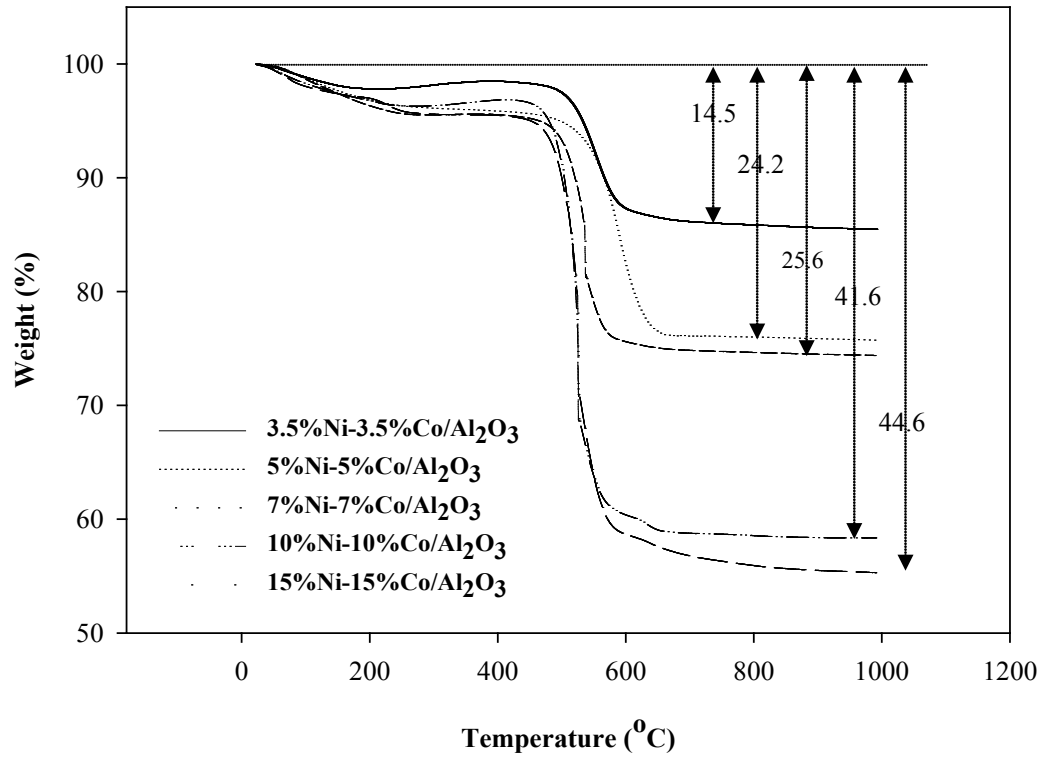

Figure 5.10 The weight loss of spent Ni-Co/Al_2O_3 bimetallic catalysts with various Ni-Co contents

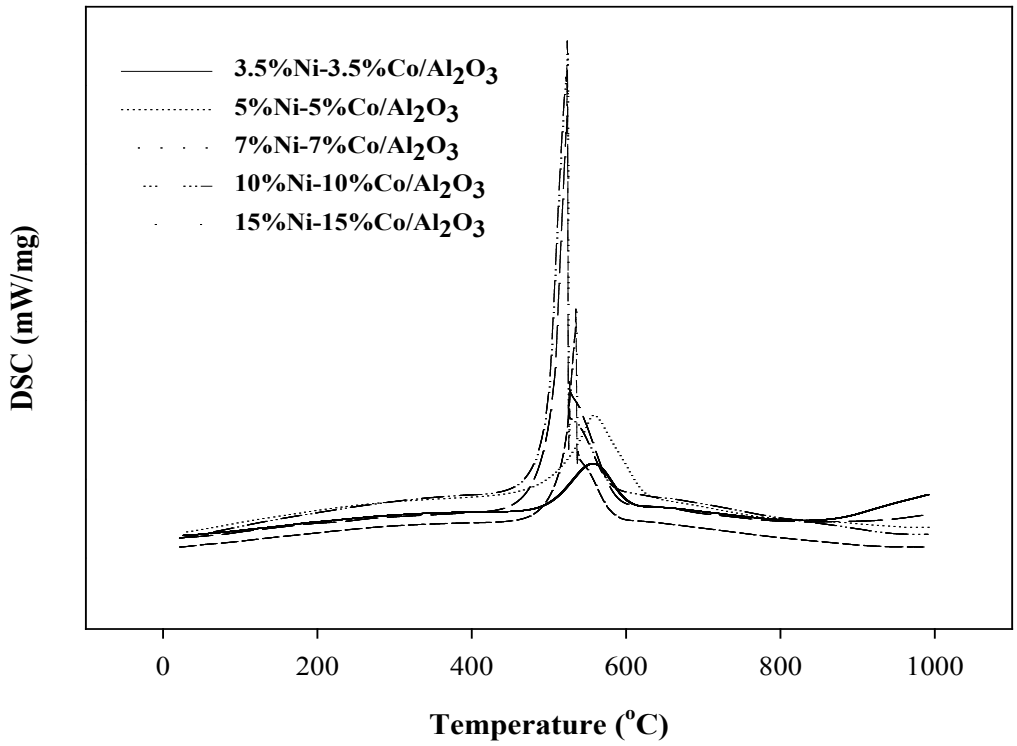

Figure 5.11 DSC curves of spent Ni-Co/Al_2O_3 bimetallic catalysts with various Ni-Co contents

5.2.2.4 Scanning electron microscopy (SEM)

The morphology of the prepared Ni-Co/Al_2O_3 bimetallic catalysts with various Ni-Co contents were 3.5wt.%Ni-3.5wt.%Co, 5wt.%Ni-5wt.%Co, 7wt.%Ni-7wt.%Co, 10wt.%Ni-10wt.%Co and 15wt.%Ni-15wt.%Co were investigated by Scanning Electron Microscopy (SEM). Figure 5.12 showed the SEM images of fresh Ni-Co/Al_2O_3 bimetallic catalysts with various Ni-Co contents. The results showed no significant differences for the shape and size of the particles. Figure 5.13 showed the SEM images of spent Ni-Co/Al_2O_3 bimetallic catalysts after 120 min reaction. It has not been found carbon deposit on 3.5wt.%Ni-3.5wt.%Co/Al_2O_3 catalyst but found many filamentous carbon on the rest. In addition, the metal particles position is very important for the catalyst stability. From the previous study found that if the particle is not covered by filament carbon, probable to accessible with the reactant gases thus

keeps the activity, on the contrary upon encapsulation the particle lose their activity due to they are not accessible to reactant gas **[48]**. In the preliminary study, it was found that the majority of filaments were presented only near the metal particle and the reaction remained stable over 120 min**.**

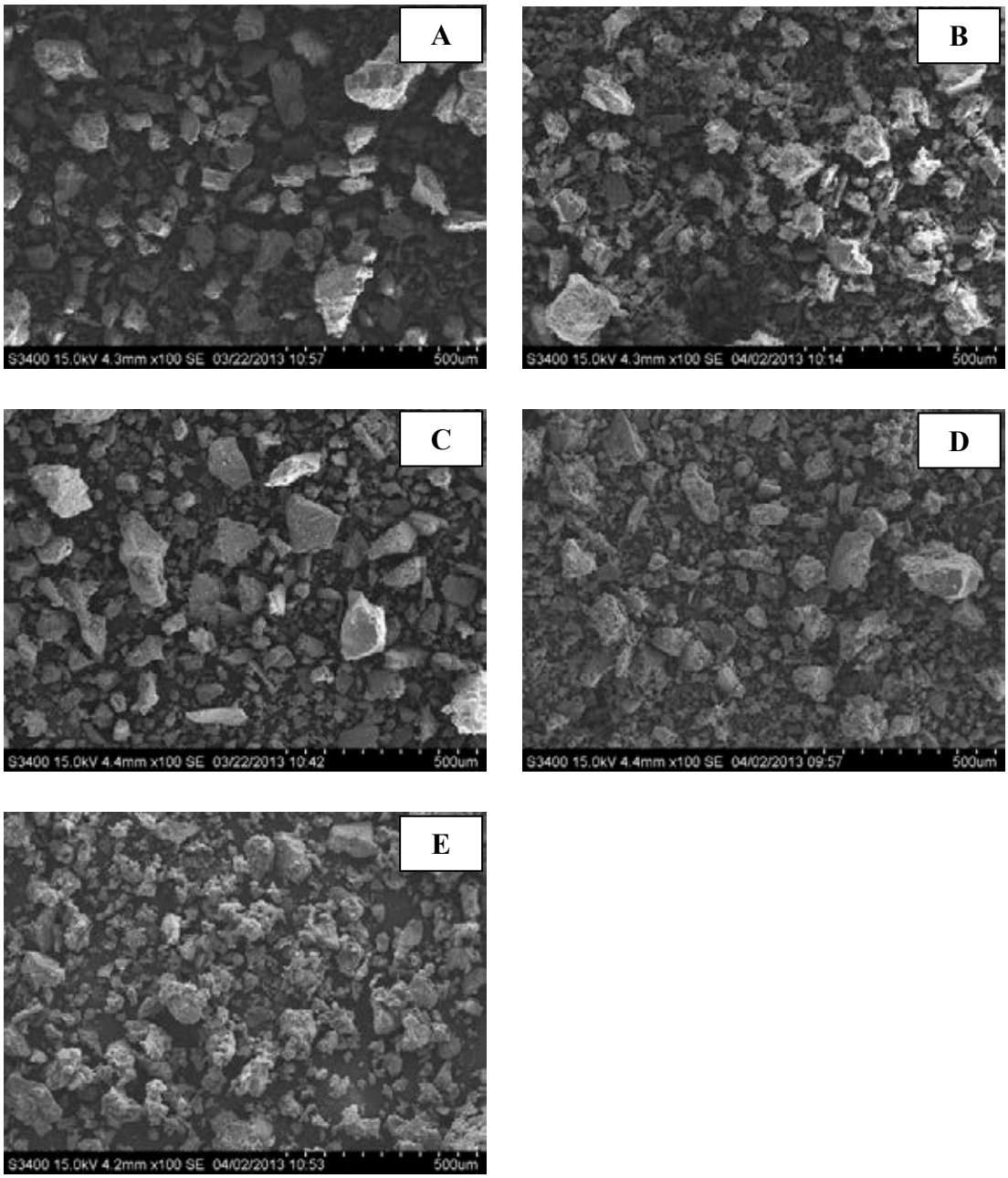

Figure 5.12 The SEM images of fresh Ni-Co/Al_2O_3 bimetallic catalysts with various Ni-Co contents, (A) 3.5%Ni-3.5%Co/Al_2O_3, (B) 5%Ni-5%Co/Al_2O_3, (C) 7%Ni-7%Co/Al_2O_3, (D) 10%Ni-10%Co/Al_2O_3, (E)15%Ni-15%Co/Al_2O_3

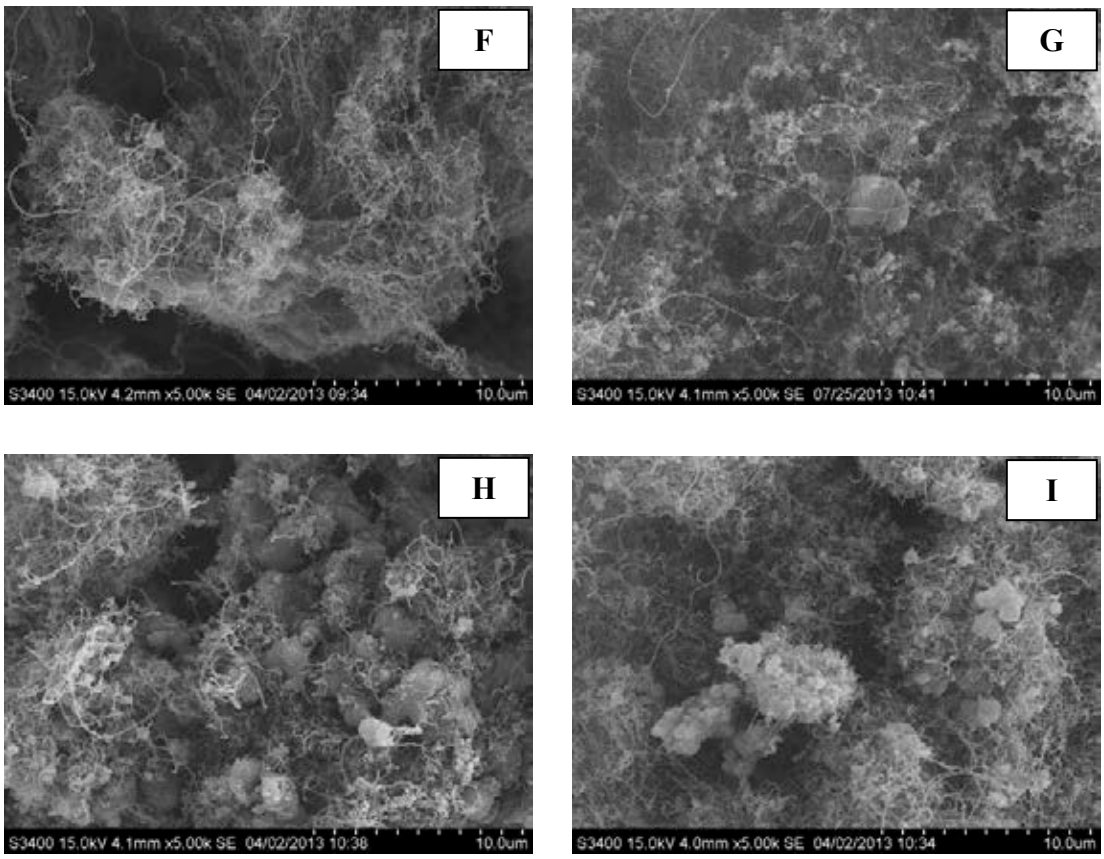

Figure 5.13 The SEM images of spent Ni-Co/Al_2O_3 bimetallic catalysts with various Ni-Co contents after 120 min reaction, (F) 5%Ni-5%Co/Al_2O_3, (G) 7%Ni-7%Co/Al_2O_3, (H) 10%Ni-10%Co/Al_2O_3, (I)15%Ni-15%Co/Al_2O_3

5.2.2.5 X-ray photoelectron spectroscopy (XPS)

XPS analysis was carried out for determining the amount of elements on the surface and the interaction between metal and supports. The supported catalysts were analyzed in the Co 2p, Ni 2p, Al 2s and O1s regarding to the binding energy regions. The binding energy of Co 2p, Ni 2p and Al 2s and the ratio of percentages of surface atomic concentration for the prepared Ni-Co/Al_2O_3 bimetallic catalysts with various Ni-Co contents are summarized in Table 5.5, indicating the binding energy of Co 2p was in the range of 780.0-781.5 eV, The binding energy for 10wt.%Ni-10wt.%Co/Al_2O_3 and 15wt.%Ni-15wt.%Co/Al_2O_3 catalysts are relevant

with Co_3O_4 whereas, the binding energy for 3.5wt.%Ni-3.5wt.%Co/Al_2O_3, 5wt.%Ni-5wt.%Co/Al_2O_3 and 7wt.%Ni-7wt.%Co/Al_2O_3 catalysts were relevant with $CoAl_2O_4$. The binding energy of Ni 2p was in the range of 855.3-858.1 eV, which all demonstration the existence of $NiAl_2O_4$, except 15wt.%Ni-15wt.%Co/Al_2O_3 catalyst was matched with of NiO. In addition, the binding energy of Al 2p was in the range of 73.9-75.9 eV. The ratios of atomic concentrations of catalysts could be observed that, the surface atomic concentration of Co and Ni on Al increasing with amount of Ni-Co contents.

Table 5.5 The binding energy and the ratio of percentages of surface atomic concentration for the prepared Ni-Co/Al_2O_3 bimetallic catalysts with various Ni-Co contents

Catalysts	**Binding energy (eV)**			**Surface atomic concentration (%)**		
	Co 2p	**Ni 2p**	**Al 2p**	**Al/O**	**Co/Al**	**Ni/Al**
3.5%Ni-3.5%Co/Al_2O_3	781.5	856.3	74.1	0.863	0.015	0.051
5%Ni-5%Co/Al_2O_3	781.1	856.6	74.7	0.827	0.019	0.059
7%Ni-7%Co/Al_2O_3	781.5	856.1	75.9	0.546	0.021	0.047
10%Ni-10%Co/Al_2O_3	780	856.5	74.3	0.397	0.246	0.278
15%Ni-15%Co/Al_2O_3	780	855.3	73.9	0.332	0.577	0.332
Co_3O_4**[52]**	780.0±0.7					
$CoAl_2O_4$**[52]**	781.9±0.5					
NiO**[57]**	855.5±0.3					
$NiAl_2O_4$**[58]**	856.8±0.6					

5.2.2.6 Temperature Programmed Desorption of Ammonia (NH_3-TPD)

The NH_3-TPD profiles of the prepared Ni-Co/Al_2O_3 bimetallic catalysts with various Ni-Co contents were 3.5wt.%Ni-3.5wt.%Co, 5wt.%Ni-5wt.%Co, 7wt.%Ni-7wt.%Co, 10wt.%Ni-10wt.%Co and 15wt.%Ni-15wt.%Co are showed in Figure 5.14. The amounts of acid sites on the surface of catalysts were calculated as showed in Table 5.6. The results found of one broad peak which at low temperature in range 100-350^{o}C for 3.5%Ni-3.5%Co and 5%Ni-5%Co bimetallic catalysts. Whereas found another one peak at higher temperature in range 350-450^{o}Cwhich had found involved with strong acid sites for 7%Ni-7%Co, 10%Ni-10%Co and 15%Ni-15%Co bimetallic catalysts. When comparing between the acidity of bimetallic catalysts and mono-metallic catalysts, bimetallic catalysts had a higher acidity than mono-metallic catalysts. This finding indicated that the increase of nickel in the cobalt-base catalysts increased the catalyst acidity.

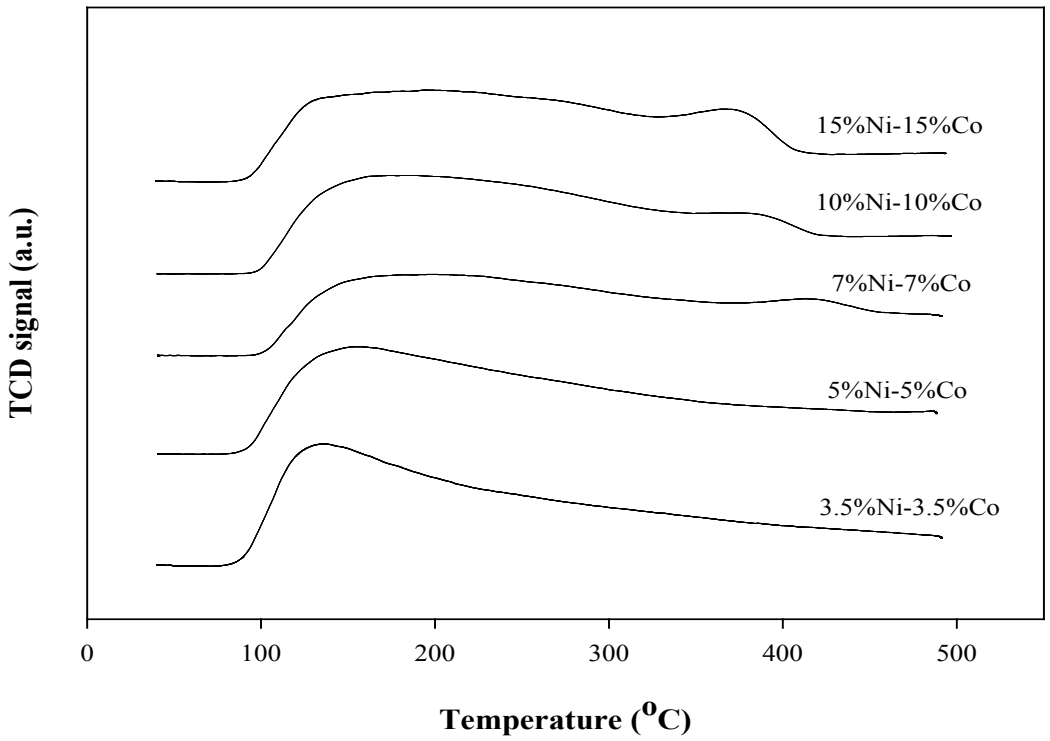

Figure 5.14 NH_3-TPD profiles of the prepared Ni-Co/Al_2O_3 bimetallic catalysts with various Ni-Co contents

Table 5.6 The acidity of the prepared Ni-Co/Al_2O_3 bimetallic catalysts with various Ni-Co contents

Catalysts	Total acid site, (mmol H^+/g)
3.5%Ni-3.5%Co/Al_2O_3	2.9670
5%Ni-5%Co/Al_2O_3	3.0389
7%Ni-7%Co/Al_2O_3	2.9205
10%Ni-10%Co/Al_2O_3	3.5334
15%Ni-15%Co/Al_2O_3	3.3187

5.3 Effect of potassium promoted 10%nickel-10%cobalt bimetallic catalysts

5.3.1 The catalytic activities in carbon dioxide reforming of methane

This section was the study of carbon dioxide reforming of methane in order to determine the catalytic activity of the prepared catalysts were $alumina_{(sol\text{-}gel)}$ supported over potassium promoted 10%nickel-10%cobalt bimetallic catalysts. The catalysts were reduced in H_2 at 600^{o}C for 1 h in a reactor. After, the reaction carried out at 700^{o}C, 1 atm with CH_4/CO_2 flow rate = 125 ml/min.

The effect of the addition of 0.1wt.% and 1wt.% potassium into 10wt.%Ni-10wt.%Co/Al_2O_3, it was found that the CH_4 conversion was slightly decreased to 91.71% and 93.76%, respectively as Figure 5.16

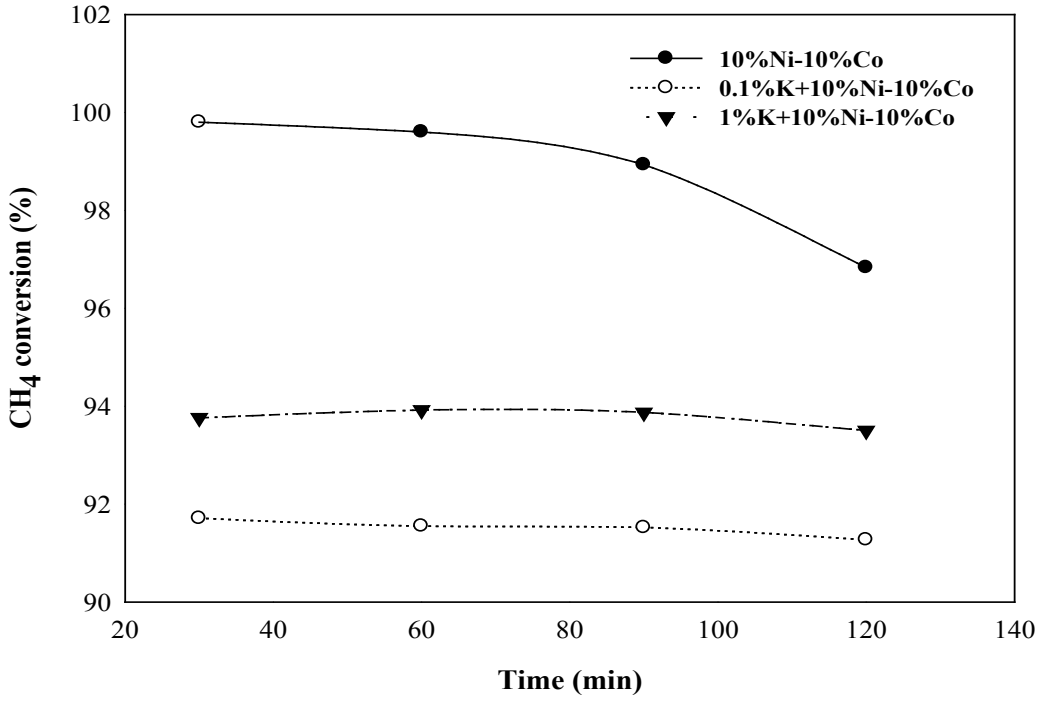

Figure 5.15 The effect of potassium promoted 10%Ni-10%Co bimetallic catalysts on the CH_4 conversion

5.3.2 Catalysts characterization

5.3.2.1 X-ray diffraction (XRD)

The crystalline phase of prepared catalysts was analyzed by X-ray diffraction (XRD). The 0.1wt.%K+10wt.%Ni-10wt.%Coand 1wt.%K+10wt.%Ni-10wt.%Co were impregnated over supported bimetallic catalyst then, after calcinations in air at 500^{o}C for 2 hours. These catalysts were tested by XRD that showed in Figure 5.16. The XRD characteristic peaks corresponding to Co_3O_4 and/or NiO were observed at $2\theta = 31^{o}$, 37^{o}, 45^{o}, 59^{o} and 65^{o} which could not be separated by XRD because their similar morphology. And at $2\theta = 46^{o}$ and 67^{o}, we found the diffraction peaks corresponding to γ-Al_2O_3. In addition, diffraction peaks of potassium did not appear in the patterns. It was possible that the potassium was highly dispersed on the catalysts.

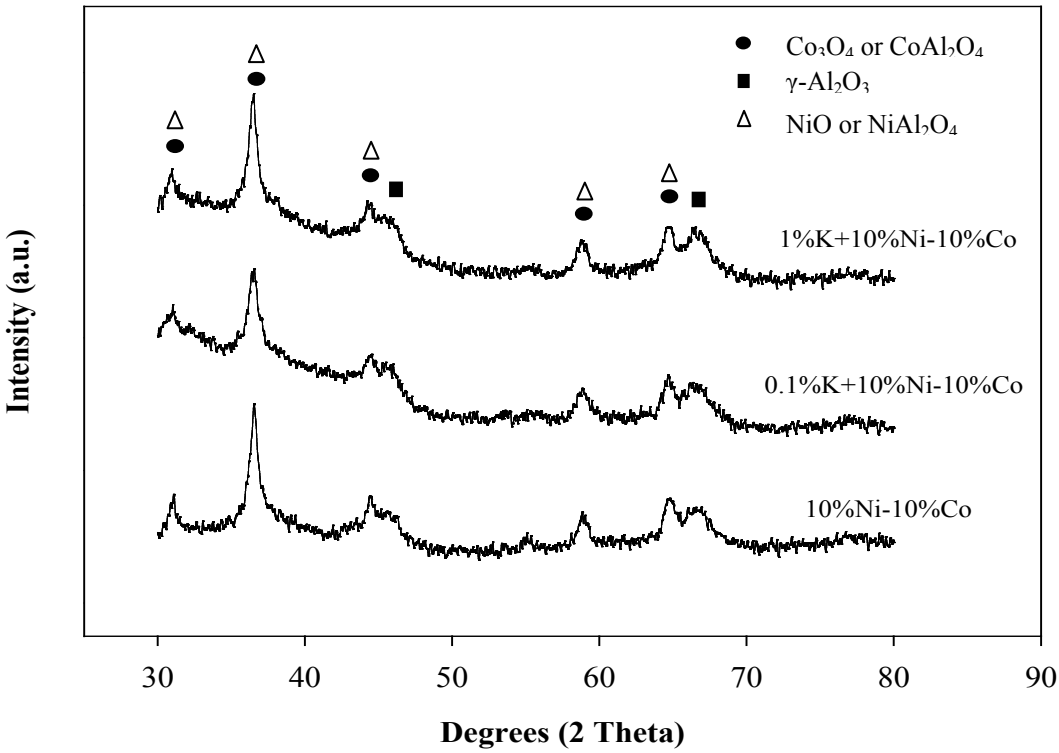

Figure 5.16 XRD patterns of the addition the potassium in 10%Ni-10%Co/Al_2O_3 bimetallic catalysts with various potassium contents

5.3.2.2 Nitrogen physisorption

BET surface area, pore volume and pore diameter of the prepared 10wt.%Ni-10wt.%Co/$Al_2O_{3(sol\text{-}gel)}$ bimetallic catalysts with addition various potassium contentswere 0.1wt.% and 1wt.% were summarized in Table 5.7. It was found that the BET surface areas of K-promoted catalysts were smaller than those of unpromoted catalyst. While it did not change significantly for pore volume and pore diameter.

Table 5.7 The BET surface area, average pore volume and average pore size of the addition various potassium contents

Catalysts	BET surface area (m^2/g)	Pore volume (cm^3/g)	Pore diameter (nm)
0.1%K+10%Ni-10%Co/Al_2O_3	111	0.22	4.79
1%K+10%Ni-10%Co/Al_2O_3	110	0.22	4.98
10%Ni-10%Co/Al_2O_3	114	0.21	5.10

5.3.2.3 Thermogravimetric analysis (TGA)

Amount of coke was determined by Thermogravimetric Analysis (TGA). Figure 5.17 showed the percent weight loss of promoted 10%Ni-10%Co/Al_2O_3 with various potassium contents were 0.1wt.% and 1wt.%. The results found that the carbon amount of promoted catalysts decrease when compared with unpromoted 10%Ni-10%Co/Al_2O_3 catalyst. Therefore, indicating the addition of potassium improved the resistance to coke formation on catalysts. This results is agree with previous research found that the potassium covers a part of active sites on catalyst therefore inhibiting the methane decomposition and consequence, decreasing both CH_4 reforming and decomposition result that decrease the carbon formation **[45]**.

Figure 5.18 showed DSC curves of spent promoted 10%Ni-10%Co/Al_2O_3 with various potassium contents were 0.1wt.% and 1wt.%. There were only one endothermic peak on the DSC curves for all catalysts which presented between 450-570^oC.

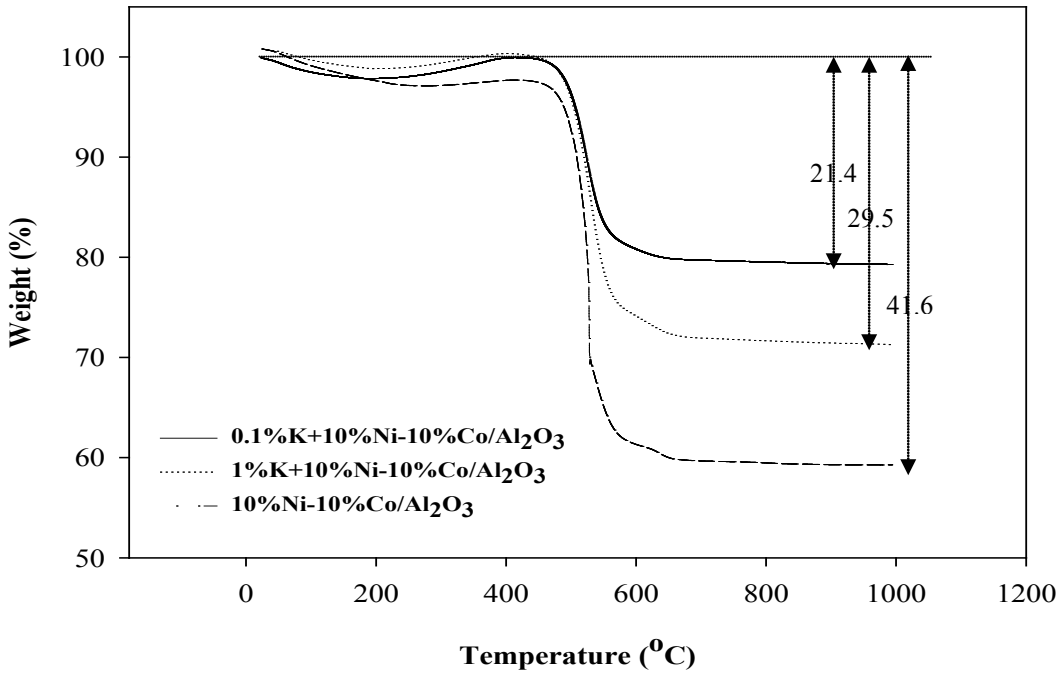

Figure 5.17 The weight loss of spent promoted 10%Ni-10%Co/Al_2O_3 bimetallic catalysts with various potassium contents

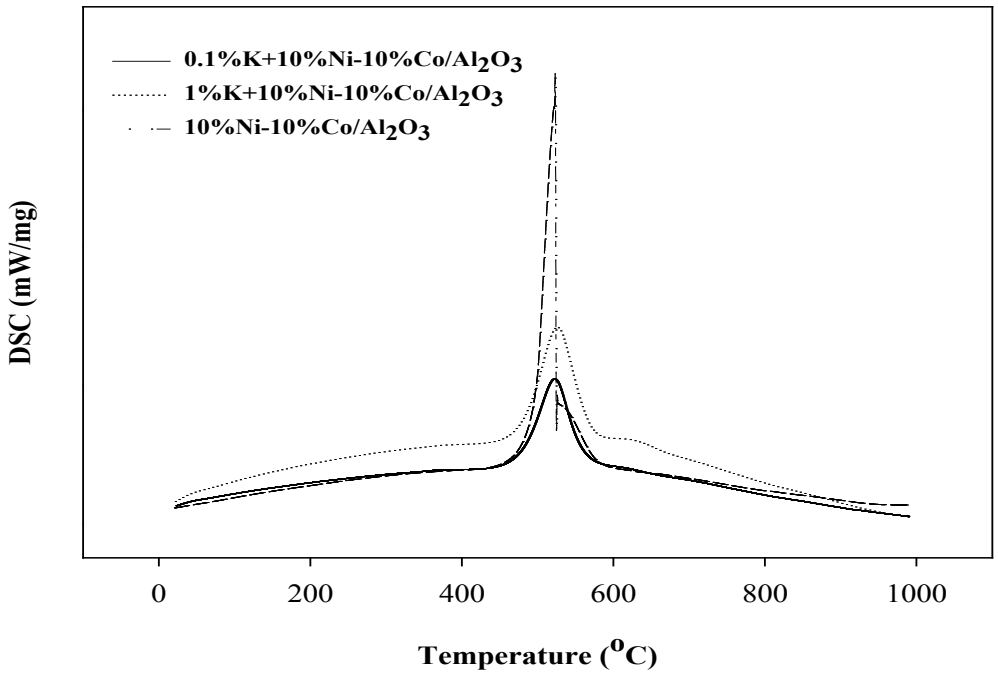

Figure 5.18 DSC curves of spent 10%Ni-10%Co/Al_2O_3 bimetallic catalysts with various potassium contents

5.3.2.4 Scanning electron microscopy (SEM)

The morphology of the prepared 10%Ni-10%Co/Al_2O_3 bimetallic catalysts with 1wt.%K was investigated by Scanning Electron Microscopy (SEM). Figure 5.19 showed the SEM images of the fresh catalysts before reaction between potassium promoted catalyst (A) and unpromoted catalyst (B). The results indicated that the changed in surface area of the catalyst with the addition of potassium. It was found the metal had distributed better for potassium promoted catalyst

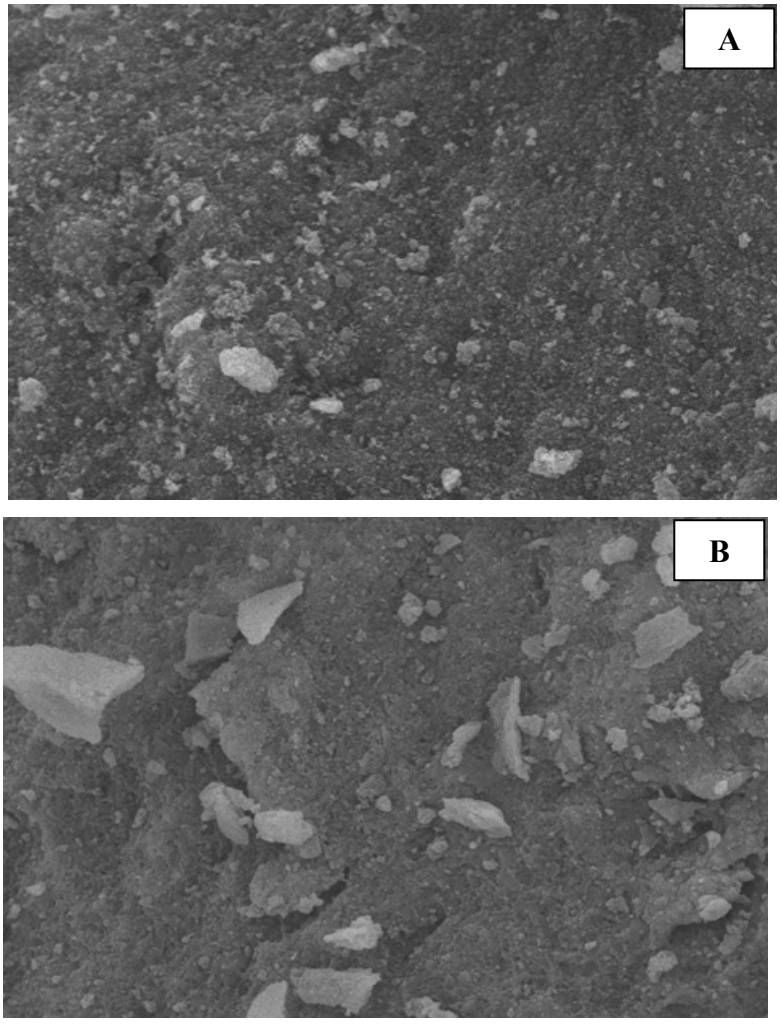

Figure 5.19 The SEM images of fresh catalysts for promoted and unpromoted catalysts, (A) promoted 10%Ni-10%Co with 1%K, (B) 10%Ni-10%Co

5.3.2.5 X-ray photoelectron spectroscopy (XPS)

XPS analysis was carried out for determined the amount of element on the surface and the interaction between metal and supports. The supported catalysts were analyzed in the Co 2p, Ni 2p, K 2p, Al 2s and O1s regarding to the binding energy regions. The binding energy of Co 2p, Ni 2p, K 2p and Al 2s and the ratio of percentages of surface atomic concentration for the addition the potassium in 10%Ni-10%Co/Al_2O_3 bimetallic catalysts with various potassium contents were summarized in Table 5.8, indicating the binding energy of Co 2p was in the range of 779.9-780.0 eV, which demonstration the existence of Co_3O_4 **[59]** corresponding with XRD, the binding energy of Ni 2p was in the range of 855.9-856.5 eV. The binding energy of Ni 2p for potassium promoted catalysts is shifted to lower than unpromoted catalyst. The binding energy of K 2p was in the range of 285.0-285.1 eV, and the binding energy of Al 2p was in the range of 74.3-75.7 eV. In addition the atomic ratio of surface concentrations of Co and Ni to Al were higher for catalysts with potassium, but it was decreased with the increasing potassium content. The higher of Co/Al and Ni/Al ratio presents in according with a higher dispersion of Co and Ni in the potassium promoted catalysts **[60]**.

Table 5.8 The binding energy and the ratio of percentages of surface atomic concentration for the addition the potassium in 10%Ni-10%Co/Al_2O_3 bimetallic catalysts with various potassium contents

Catalysts	Binding energy (eV)				Surface atomic concentration (%)			
	Co 2p	Ni 2p	K 2p	Al 2p	Al/O	K/Al	Co/Al	Ni/Al
0.1%K+10%Ni-10%Co/Al_2O_3	780	855.9	285.1	75.7	0.366	0.253	0.347	0.475
1%K+10%Ni-10%Co/Al_2O_3	779.9	856.1	285	75.6	0.399	0.184	0.298	0.337
10%Ni-10%Co/Al_2O_3	780	856.5	-	74.3	0.397	-	0.246	0.278

Co_3O_4: 780.0±0.7 eV, $CoAl_2O_4$: 781.9±0.5 eV **[52]**

NiO: 855.5±0.3 eV, $NiAl_2O_4$: 856.8±0.6 eV **[57-58]**

5.3.2.6 Temperature Programmed Desorption of Ammonia (NH_3-TPD)

The NH_3-TPD profiles of the addition the potassium in 10%Ni-10%Co/Al_2O_3 bimetallic catalysts with various potassium contents were showed in Figure 5.20. From NH_3-TPD profiles, we can calculate the amount of acid sites on the surface of catalysts as showed in Table 5.9. The results showed one broad peak at low temperature in range 100-350^oC which corresponded to the weak acid sites for all prepared catalysts. With the addition of potassium on supported catalysts, the amount of acid sites was decreased significantly. This result agrees with the previous research which said the higher acidity catalyst increase the chances of carbon formation on the surface catalysts **[61]**. The results of the TGA also showed the weight loss that noticeably decreased for the K-promoted catalysts.

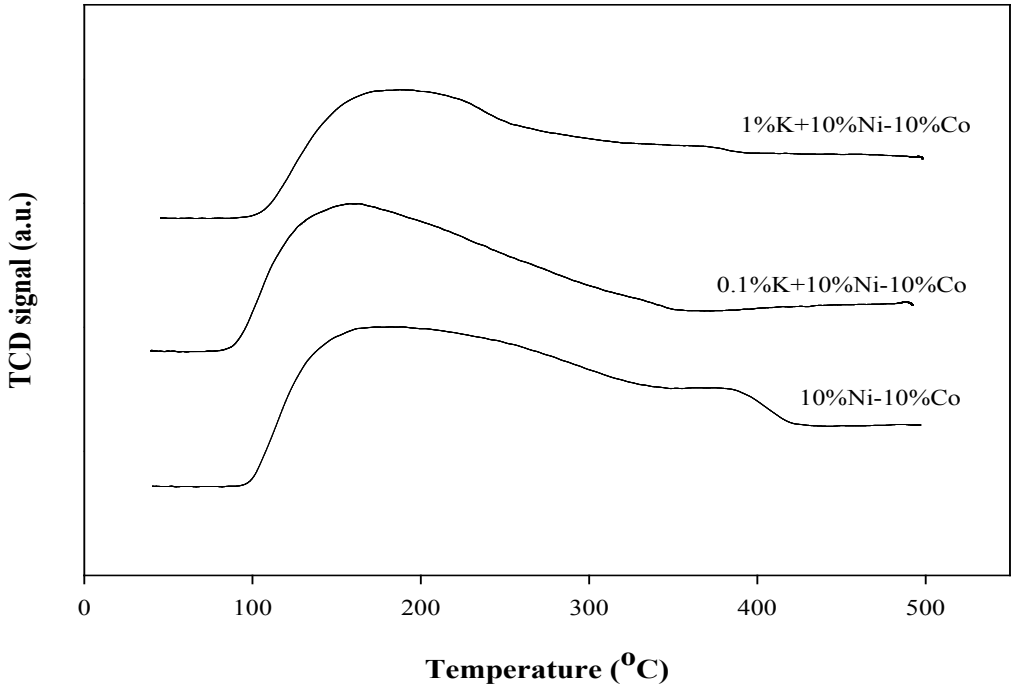

Figure 5.20 NH_3-TPD profile of the addition the potassium in 10%Ni-10%Co/Al_2O_3 bimetallic catalysts with various potassium contents

Table 5.9 The acidity of the addition the potassium in 10%Ni-10%Co/Al_2O_3 bimetallic catalysts with various potassium contents

Catalysts	**Total acid site (mmol H^+/g)**
0.1%K+10%Ni-10%Co/Al_2O_3	3.1645
1%K+10%Ni-10%Co/Al_2O_3	3.2499
10%Ni-10%Co/Al_2O_3	3.5334

CHAPTER VI
CONCLUSION AND RECOMMENDATIONS

6.1 Conclusions

In this research studied the carbon dioxide reforming of methane reaction using cobalt mono-metallic catalysts, nickel-cobalt bimetallic catalysts and potassium promoted 10wt.%Ni-10wt.%Co over alumina supported. The results can be concluded that after 120 minutes reaction, the catalysts that gave the best methane conversion were 10wt.%Co/Al_2O_3 for mono-metallic catalysts and 10wt.%Ni-10wt.%Co/Al_2O_3 for bimetallic catalysts, which were 61.86% and 96.86% respectively. Moreover, the effect adding potassium promoter to 10wt.%Ni-10wt.%Co/Al_2O_3 catalyst was studied. The methane conversion of potassium promoted 10wt.%Ni-10wt.%Co/Al_2O_3 catalyst was slightly lower than one without potassium. However, the adding of promoter could significantly decrease the carbon content on the catalysts.

6.2 Recommendations

For this experiment can be improved in the future as follows.

1) To study the effect of the long time reaction on activity and stability of catalysts.
2) To study the effect of using the various proportions in bimetallic catalysts.

REFERENCES

[1] Turner et al. Renewable hydrogen production. Int J Energy Res 32 (2008): 379-407.

[2] Garciaa, V.; Fernandeza, J.J.; Ruiza, W.; Mondragona, F.; and Moreno, A. Effect of MgO addition on the basicity of Ni/ZrO_2 and on its catalytic activity in carbon dioxide reforming of methane. Catalysis Communications 11 (2009): 240–246.

[3] Ozkara-Aydınoglu, S.; Ozensoy, E.; and Aksoylu, A.E. The effect of impregnation strategy on methane dry reforming activity of Ce promoted Pt/ZrO_2. International Journal of Hydrogen Energy 34 (2009): 9711–9722.

[4] Zhang, K.; Zhou, G.; Li, J.; and Cheng, T. The electronic effects of Pr on $La_{1-x}Pr_xNiAl_{11}O_{19}$ for CO_2 reforming of methane. Catalysis Communications 10 (2009): 1816–1820.

[5] Zhao, Y.; Pan, Y.X.; Xie, Y.; and Liu, C.J. Carbon dioxide reforming of methane over glow discharge plasma-reduced Ir/Al_2O_3 catalyst. Catalysis Communications 9 (2008): 1558–1562.

[6] Guo, J.; Hou, Z.; Gao, J.; and Zheng, X. Syngas production via combined oxy-CO_2 reforming of methane over Gd_2O_3-modified Ni/SiO_2 catalyst in a fluidized-bed reactor. Fuel 87 (2008): 1348-1354.

[7] Ruckenstein, E. and Wang, H.Y. Carbon deposition and catalytic deactivation during CO_2 reforming of CH_4 over Co/γ-Al_2O_3 Catalysts. Journal of Catalysis 205 (2002): 289-293.

[8] Gao, J.; Hou, Z.; Guo, J.; Zhu, Y.; and Zheng, X. Catalytic conversion of methane and CO_2 to synthesis gas over a La_2O_3-modified SiO_2 supported Ni catalyst in fluidized-bed reactor. Catalysis Today 131 (2008): 278-284.

[9] Therdthianwong, S.; Therdthianwong, A.; Siangchin, C.; and Yongprapat, S. Synthesis gas production from dry reforming of methane over Ni/Al_2O_3 stabilized by ZrO_2. International journal of hydrogen energy 33 (2008): 991-999.

[10] Pawelec, B.; Damyanova, S.; Arishtirova, K.; Fierro, J.; and Petrov, L. Structural and surface features of Pt Ni catalysts for reforming of methane with CO_2. Applied Catalyst A 323 (2007): 188-201.

[11] Sahli, N.; Petit, C.; Roger, A.; Kiennemann, A.; Libs, S.; and Bettahar, M. Ni catalysts from $NiAl_2O_4$ spinel for CO_2 reforming of methane. Catalysis Today 113 (2006): 187-193.

[12] Wang, N.; Chu, W.; Huang, L.; and Zhang, T. Effects of Ce/Zr ratio on the structure and performances of Co-$Ce_{1-x}Zr_xO_2$ catalysts for carbon dioxide reforming of methane. Journal of Natural Gas Chemistry 19 (2010): 117-122.

[13] Wei, J. and Iglesia, E. Isotopic and kinetic assessment of the mechanism of reactions of CH_4 with CO_2 or H_2O to form synthesis gas and carbon on nickel catalysts. Journal of Catalysis 224 (2004): 370-383.

[14] Pechimuthu, N.A.; Pant, K.K.; Dhingra, S.C.; and Bhalla, R. Ind. Eng. Chem. Res. 45 (2006): 7435–7443.

[15] Bradford, M. C. J. and Vannice, M. A. Journal of Catalysis 173 (1998): 157–171.

[16] Richardson, J. T.; Garrait, M.; and Hung, J. K. Applied catalyst A 255 (2003): 69–82.

[17] Ozkera-Aydinoglu, S. and Aksoylu, A.E. CO_2 reforming of methane over Pt-Ni/Al_2O_3 catalysts: Effect of catalyst composition, and water and oxygen addition to the feed. International journal of hydrogen energy 36 (2011): 2950-2959.

[18] Ozkara-Aydınoglu, S. and Aksoylu, A.E. Carbon dioxide reforming of methane over Co-X/ZrO_2 catalysts (X=La, Ce, Mn, Mg, K). Catalysis communications 11 (2010): 1165–1170.

[19] Zhang, J.G.; Wang, H.; and Ajay, K.D. Development of stable bimetallic catalysts for carbon dioxide reforming of methane. Journal of Catalysis 249 (2007): 300–310.

[20] Topalidis, A.; Petrakis, D.E.; Ladavos, A.; Loukatzikou, L.; and Pomonis, P.J. Catalyst Today 127 (2007): 238–245.

[21] Fan, M.S.; Abdullah, A.Z.; and Bhatia, S. Catalytic Technology for Carbon Dioxide Reforming of Methane to Synthesis Gas. ChemCatChem 1 (2009): 192–208.

[22] Zeng, S.; Zhang, L.; Zhang, X.; Wang, Y.; Pan, H.; and Su H. Modification effect of natural mixed rare earths on Co/γ-Al_2O_3 catalysts for CH_4/CO_2 reforming to synthesis gas. International Journal of hydrogen energy 37 (2012): 9994-10001.

[23] Loeng, R.; Bjogum, E.; Enger, BC.; Eilertsen, JL.; Holmen, A.; Krogh, B., et al. Catalytic partial oxidation of CH_4 to H_2 over cobalt catalysts at moderate temperatures. Applied catalyst A 333 (2007): 11-23.

[24] Ruckenstein, E. and Wang, HY. Carbon dioxide reforming of methane to synthesis gas over supported cobalt catalysts. Applied catalyst A 204 (2000): 257-263.

[25] Koh, ACW.; Chen, L.; Leong, WK.; Johnson, BFG.; Khimyak, T.; and Lin, J. Hydrogen or synthesis gas production via the partial oxidation of methane over supported nickel-cobalt catalysts. International journal of hydrogen energy 32 (2007): 725-730.

[26] Hawkins, M. Why we need cobalt. Applied Earth Science: Transactions of the Institution of Mining & Metallurgy, Section B 110 (2001): 66-71.

[27] Khodakov, Y.A.; Chu, W.; and Fongarland, P. Advances in the Development of Novel Cobalt Fischer-Tropsch catalysts for synthesis of Long-Chain Hydrocarbons and Clean Fuels. Chemical review 107 (2007): 1692-1744.

[28] Othmer, K. Encyclopedia of chemical technology. Vol 6. 4th ed. New York: A Wiley Interscience Publication, John Wiley&Son, 1991.

[29] Oberlander, R.K. Aluminus for catalysts, in Applied Industrial catalysis, ed. B.E.Leach. Academic Press, vol.3 chapter 4. 1984.

[30] Nuchchanok Yoonpan. Reforming reaction of methane by carbon dioxide over supported nickel catalysts. Master's Thesis, Department of Chemical Engineering Engineering Chulalongkorn University. 2008.

[31] Brinker, C.J.; Hurd, A.J.; Schunk, P.R.; Frye, G.C.; and Ashley, C.S. Review of sol-gel thin film formation. Journal of Non-Crystalline Solids 147-148 (1992): 424-436.

[32] Joongjai Panpranot. Fundamentals of heterogeneous catalysts. Bangkok: Department of Chemical Engineering Chulalongkorn University, 2011.

[33] Chen, J.; Yao, C.; Zhao, Y.; and Jia, P. Synthesis gas production from dry reforming of methane over $Ce_{0.75}Zr_{0.25}O_2$-supported Ru catalysts. International journal of hydrogen energy 35 (2010): 1630–1642.

[34] Kohn, M.P.; Castaldi, M.J.; and Farrauto, R.J. Auto-thermal and dry reforming of landfill gas over a Rh/ɣ-Al_2O_3 monolith catalyst. Applied Catalysis B: Environmental 94 (2010): 125–133.

[35] San Jose-Alonso, D.; Illan-Gomez, M.J.; and Roman-Martınez, M.C. Low metal content Co and Ni alumina supported catalysts for the CO_2 reforming of methane. International journal of hydrogen energy 38 (2013): 2230-2239.

[36] Adolfo E. Castro Luna and Marıa E. Iriarte. Carbon dioxide reforming of methane over a metal modified Ni-Al_2O_3 catalyst. Applied Catalysis A: General 343 (2008): 10–15.

[37] Takanabe, K.; Nagaoka, K.; Nariai, K.; and Aika, K. Influence of reduction temperature on the catalytic behavior of Co/TiO_2 catalysts for CH_4/CO_2 reforming and its relation with titania bulk crystal structure. Journal of Catalysis 230 (2005): 75–85.

[38] Ruckenstein, E. and Wang, H.Y. Carbon deposition and catalytic deactivation during CO_2 reforming of CH_4 over Co/ɣ-Al_2O_3 catalysts. Journal of Catalysis 205 (2002): 289–293.

[39] Fidalgo, B.; Zubizarreta, L.; Bermúdez, J.M.; Arenillas, A.; and Menéndez, J.A. Synthesis of carbon-supported nickel catalysts for the dry reforming of CH_4. Fuel Processing Technology 91 (2010): 765–769.

[40] Omata, K.; Nukui, N.; Hottai, T.; Showa, Y.; and Yamada, M. Strontium carbonate supported cobalt catalyst for dry reforming of methane under pressure. Catalysis Communications 5 (2004): 755–758.

[41] Nagai, M.; Nakahira, K.; Ozawa, Y.; Namiki, Y.; and Suzuki, Y. CO_2 reforming of methane on Rh/Al_2O_3 catalyst. Chemical Engineering Science 62 (2007): 4998 – 5000.

[42] Wang, H.Y. and Ruckenstein, E. Carbon dioxide reforming of methane to synthesis gas over supported rhodium catalysts: the effect of support. Applied Catalysis A: General 204 (2000): 143–152.

[43] Ji, L.; Tang, S.; Zeng, H.C.; Lin, J.; and Tan, K.L. CO_2 reforming of methane to synthesis gas over sol–gel-made $Co/\gamma\text{-}Al_2O_3$ catalysts from organometallic precursors. Applied Catalysis A: General 207 (2001): 247–255.

[44] Wang, N.; Chua, W.; Zhang, T.; and Zhao, X.S. Manganese promoting effects on the $Co–Ce–Zr–O_x$ nano catalysts for methane dry reforming with carbon dioxide to hydrogen and carbon monoxide. Chemical Engineering Journal 170 (2001): 457–463.

[45] San Jose-Alonso, D.; Illan-Gomez, M.J.; and Roman-Martinez, M.C. K and Sr promoted Co alumina supported catalysts for the CO2 reforming of methane. Catalysis Today 176 (2011): 187– 190

[46] Adolfo E. Castro Luna and María E. Iriarte. Carbon dioxide reforming of methane over a metal modified $Ni\text{-}Al_2O_3$ catalyst. Applied Catalysis A: General 343 (2008): 10–15

[47] Nagaraja, B.M.; Bulushev, D.A.; Beloshapkin, S.; and Julian R.H. Ross. The effect of potassium on the activity and stability of $Ni–MgO–ZrO_2$ catalysts for the dry reforming of methane to give synthesis gas. Catalysis Today 178 (2011): 132– 136

[48] San-Jose-Alonso, D.; Juan-Juan, J.; Illan-Gomez, M.J.; and Roman-Martınez, M.C. Ni, Co and bimetallic Ni–Co catalysts for the dry reforming of methane. Applied Catalysis A: General 371 (2009): 54–59.

[49] Takanabe, K.; Nagaoka, K.; Nariai, K.; and Aika, K. Titania-supported cobalt and nickel bimetallic catalysts for carbon dioxide reforming of methane. Journal of Catalysis 232 (2005): 268–275.

[50] Zhang, J.; Wang, H.; and Dalai, A.K. Effects of metal content on activity and stability of Ni-Co bimetallic catalysts for CO_2 reforming of CH_4. Applied Catalysis A: General 339 (2008): 121–129.

[51] Natpakan Srisawad. Preparation of Co/Al_2O_3 catalysts by solid-state reaction between gibbsite and various cobalt precursors. Master's Thesis, Department of Chemical Engineering Engineering Chulalongkorn University. 2010.

[52] Tomishige, K.; Yamazaki, O.; Chen, Y.G.; Yokoyama, K.; Li, X.H.; Fujimoto, K. Development of ultra-stable Ni catalysts for carbon dioxide reforming of methane. Catalysis Today 45 (1998): 35-39.

[53] Orapin Chokpaisan. Effect of Gallium-modified Al_2O_3 TiO_2 and SiO_2 supports on characteristics and catalytic properties of supported cobalt catalysts. Master's Thesis, Department of Chemical Engineering Engineering Chulalongkorn University. 2008.

[54] Han, S.J.; Bang, Y.; Jeong Gil Seo, Yoo, J.; and Song, I. K. Hydrogen production by steam reforming of ethanol over mesoporous $Ni-Al_2O_3-ZrO_2$ xerogel catalysts: Effect of Zr/Al molar ratio. International journal of hydrogen energy 38 (2013): 1376-1383.

[55] Heracleous, E.; Lee, A.F.; Wilson, K.; and Lemonidou, A.A. Investigation of Ni-based alumina-supported catalysts for the oxidative dehydrogenation of ethane to ethylene: structural characterization and reactivity studies. Journal of Catalysis 231 (2005): 159–171.

[56] Zhang, J.; Wang, H.; and Dalai, A.K. Effects of metal content on activity and stability of Ni-Co bimetallic catalysts for CO_2 reforming of CH_4. Applied Catalysis A: General 339 (2008): 121–129.

[57] Hwang, S. et al. Hydrogenation of carbon monoxide to methane over mesoporous nickel-M-alumina (M = Fe, Ni, Co, Ce, and La) xerogel catalysts. Journal of Industrial and Engineering Chemistry 18 (2012): 243–248.

[58] Xiang, L.; Gong, Y.L..; Li, J.C.; and Wang, Z.W. Influence of hydrothermal modification on the properties of Ni/Al_2O_3 catalyst. Applied Surface Science 239 (2004): 94–100.

[59] Ji, L.; Lin, J.; and Zeng, C.H. Metal support interactions in Co/Al_2O_3 catalysts: A comparative study on reactivity of support. The Journal of Physical Chemistry 104 (2000): 1783-1790.

[60] Juan-Juan, J.; Roman-Martınez, M.C.; and Illan-Gomez, M.J. Effect of potassium content in the activity of K-promoted Ni/Al_2O_3 catalysts for the dry reforming of methane. Applied Catalysis A: General 301 (2006): 9–15.

[61] Yu, J.; Ge, Q.; Fang, W.; and Xu, H. Enhanced performance of Ca-doped Pt/γ-Al_2O_3 catalyst for cyclohexane dehydrogenation. International journal of hydrogen energy 36 (2011): 11536-11544.

APPENDICES

APPENDIX A
CALCULATION FOR CATALYST PREPARATION

1. Preparation of Co/Al_2O_3 catalyst by impregnation

Preparation of Co/Al_2O_3 catalysts by impregnation method with various cobalt contents were 7%, 10% and 15% that showed as follows:

Example : Preparation of the 7wt.%Co/Al_2O_3 catalyst

Reagent:	$Co(No_3)_2.6H_2O$,	Molecular weight	=	292 g/mol
	Co,	Molecular weight	=	59 g/mol

At 1 gram catalyst, consisted of:	Alumina	=	0.93	g
	Cobalt	=	0.07	g

Calculation:

$$Co(No_3)_2.6H_2O = \frac{0.07 \times 292}{59} = 0.3464 \text{ g}$$

Thus, the 7%CO/Al_2O_3 catalyst was prepared from the 0.3464 g of $Co(NO_3)_2.6H_2O$ impregnated on 0.93 g of $alumina_{(sol\text{-}gel)}$ supported.

2. Preparation of Ni-Co/Al_2O_3 bimetallic catalyst by co-impregnation

Preparation of Ni-Co/Al_2O_3 bimetallic catalysts by co-impregnation method with various nickel-cobalt contents were 3.5%-3.5%, 5%-5%, 7%-7%, 10%-10% and 15%-15% that showed as follows:

Example : Preparation of the 3.5wt.%Ni-3.5wt.%Co/Al_2O_3 catalyst

Reagent:	$Ni(No_3)_2.6H_2O$,	Molecular weight	=	292 g/mol
	Ni,	Molecular weight	=	59 g/mol
	$Co(No_3)_2.6H_2O$,	Molecular weight	=	292 g/mol
	Co,	Molecular weight	=	59 g/mol

At 1 gram catalyst, consisted of:	Alumina	=	0.93 g
	Nickel	=	0.035 g
	Cobalt	=	0.035 g

Calculation:

$$Ni(No_3)_2.6H_2O = \frac{0.035 \times 292}{59} = 0.1732 \text{ g}$$

$$Co(No_3)_2.6H_2O = \frac{0.035 \times 292}{59} = 0.1732 \text{ g}$$

Thus, the 3.5wt.%Ni-3.5wt.%Co/Al_2O_3 bimetallic catalyst was prepared from the 0.1732 g of $Ni(NO_3)_2.6H_2O$ and 0.1732 g of $Co(NO_3)_2.6H_2O$ impregnated on 0.93 g of $alumina_{(sol\text{-}gel)}$ supported.

3. Preparation of potassium promoted Ni-Co/Al_2O_3 catalyst by co-impregnation

Preparation of potassium promoted 10wt.%Ni-10wt.%Co/Al_2O_3 bimetallic catalysts by co-impregnation method with various potassium contents were 0.1wt.% and 1wt.% that showed as follows:

Example : Preparation of the 0.1wt.%K promoted 10wt.%Ni-10wt.%Co/Al_2O_3 bimetallic catalyst

Reagent:	$Ni(No_3)_2.6H_2O$,	Molecular weight	=	292 g/mol
	Ni,	Molecular weight	=	59 g/mol
	$Co(No_3)_2.6H_2O$,	Molecular weight	=	292 g/mol
	Co,	Molecular weight	=	59 g/mol
	KNO_3,	Molecular weight	=	101 g/mol
	K,	Molecular weight	=	39 g/mol

At 1 gram catalyst, consisted of:	Alumina	=	0.799 g
	Nickel	=	0.1 g
	Cobalt	=	0.1 g
	Potassium	=	0.001 g

Calculation:

$$Ni(No_3)_2.6H_2O = \frac{0.1 \times 292}{59} = 0.4949 \text{ g}$$

$$Co(No_3)_2.6H_2O = \frac{0.1 \times 292}{59} = 0.4949 \text{ g}$$

$$KNO_3 = \frac{0.001 \times 101}{39} = 0.0026 \text{ g}$$

Thus, the 0.1wt.%K promoted 10wt.%Ni-10wt.%Co/Al_2O_3 bimetallic catalyst was prepared from the 0.4949 g of $Ni(NO_3)_2.6H_2O$, 0.4949 g of $Co(NO_3)_2.6H_2O$ and 0.0026 g of KNO_3 impregnated on 0.799 g of $alumina_{(sol\text{-}gel)}$ supported.

APPENDIX B
CALIBRATION CURVES

This appendix shows the calibration curves for calculation of composition of products and reactants in reforming reaction of methane by carbon dioxide over supported cobalt catalysts, nickel-cobalt bimetallic catalysts and potassium promoted 10wt.%Ni-10wt.%Co/Al_2O_3 bimetallic catalysts. The main products of this reaction are carbon monoxide and hydrogen.

The Thermal Conductivity Detector (TCD), gas chromatography Shimadzu model 8A was used to analyze the concentration of products and reactants by using molecular sieve 5A and porapack-Q column.

Mole of reagent in y-axis and area reported by gas chromatography in x-axis are exhibited in the curves. The calibration curves of carbon dioxide, methane, hydrogen and carbon monoxide are illustrated in Figure B1-B4, respectively.

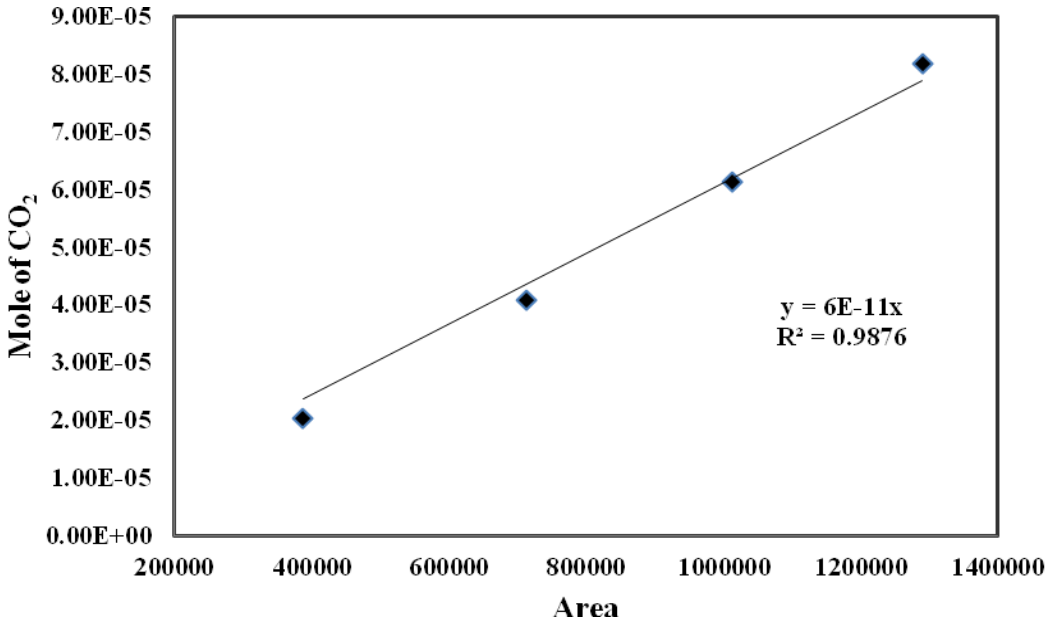

Figure B.1 The calibration curve of carbon dioxide

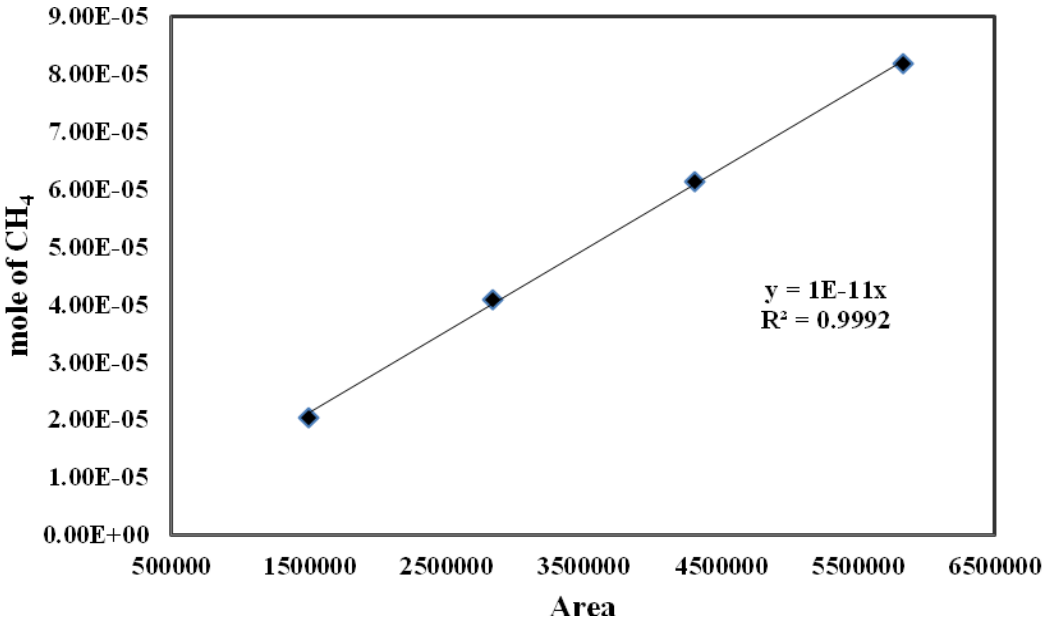

Figure B.2 The calibration curve of methane

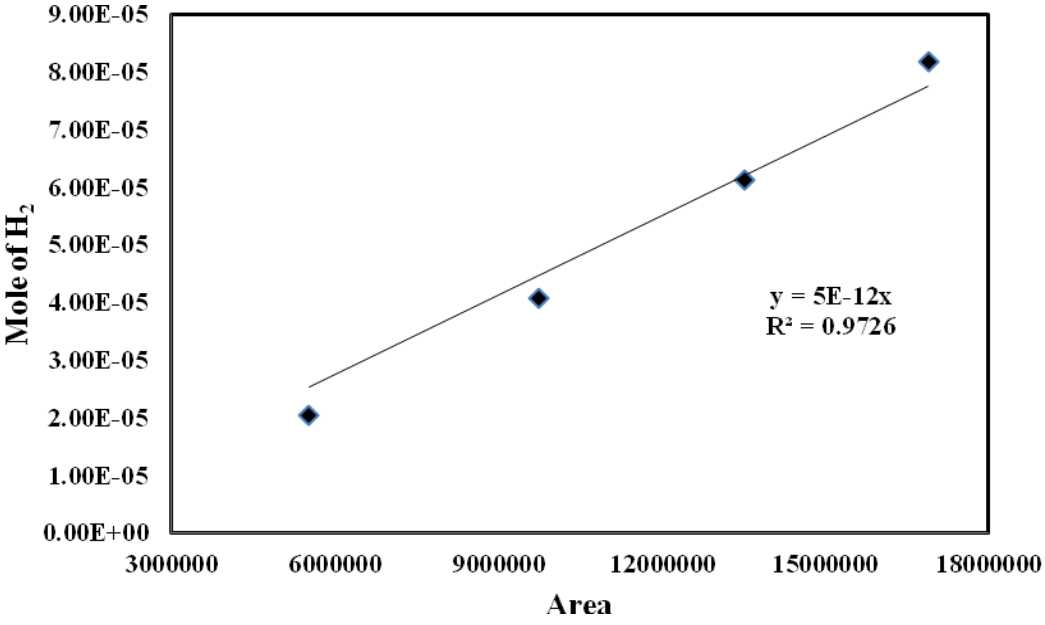

Figure B.3 The calibration curve of hydrogen

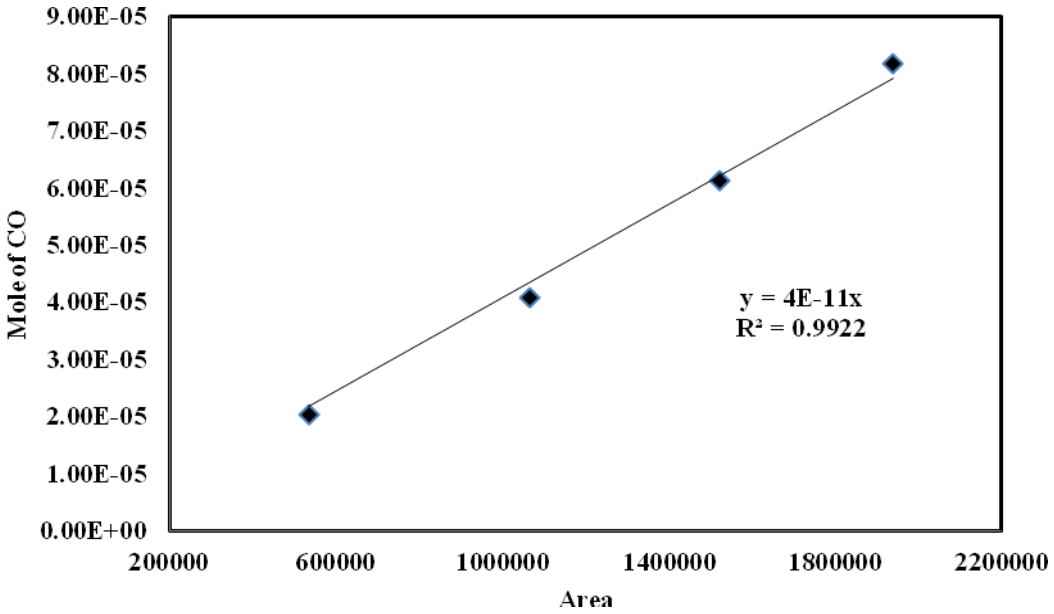

Figure B.4 The calibration curve of carbon monoxide

APPENDIX C
DATA FOR CALCULATION OF ACID SITE

Calculation of total acid sites

The total acid site of prepared catalyst is calculated as follows.

1. Conversion of total peak area to peak volume

Conversion from Micromeritrics Chemisorb 2750 is equal to 77.57016 ml/area unit. Therefore, total peak volume is derived from

Example: The $Al_2O_{3\ (sol\text{-}gel)}$ supported has the total peak area equal to 0.60536

Total peak volume = 77.57016 × total peak area

= 77.57016 × 0.833

= 64.6159 ml

2. Calculation for adsorbed volume of 15% NH_3

Adsorbed volume of 15% NH_3 = 0.15 × total peak volume

= 0.15 × 64.6159 ml

= 9.6924 ml

3. Total acid sites are calculated from the following equation

$$\text{Total acid sites} = \frac{(Adsorbed\ volume, ml) \times 101.325\, Pa}{8.314 \frac{Pa \cdot ml}{K \cdot mmol} \times 298\, K \times (weight\ of\ catalyst, g)}$$

For the $Al_2O_{3\ (sol\text{-}gel)}$ supported, used 0.1005 g of this sample was measured. Therefore;

$$\text{Total acid site} = \frac{9.6924\, ml \times 101.325\, Pa}{8.314 \frac{Pa \cdot ml}{K \cdot mmol} \times 298\, K \times (0.1005\, g)}$$

$$= 3.9442 \text{ mmol } H^+/g$$

APPENDIX D
LIST OF PUBLICATION

Waralee Marungrueang and Suphot Phatanasri "Dry reforming of methane reaction for hydrogen and syngas production using cobalt catalysts and nickel-cobalt bimetallic catalysts", The 5th Rajamangala University of Technology International Conference (5th RMUTIC), Bangkok, Thailand, July, 15-16, 2013.

VITA

Miss Waralee Marungrueang was born on May 13rd, 1987 in Bangkok, Thailand. She finished high school from Matthayom Wat Nongkeam School in 2003, and received the bachelor's degree of Chemical Engineering Srinakarin Wirot University in 2008. She continued her master's degree at Department of Chemical Engineering, Faculty of Engineering, Chulalongkorn University in December, 2010.